4-2006

Computational Simulation of Turbulent Forced Convection Flow over a Horizontal Plate Heater in a Rectangular Channel

Bhagavathi Perumal Natarajan

COMPUTATIONAL SIMULATION OF TURBULENT FORCED CONVECTION FLOW OVER A HORIZONTAL PLATE HEATER IN A RECTANGULAR CHANNEL

by

Bhagavathi Perumal Natarajan

A Thesis
Submitted to the
Faculty of The Graduate College
in partial fulfillment of the
requirements for the
Degree of Master of Science in Engineering (Mechanical)
Department of Mechanical and Aeronautical Engineering

Western Michigan University
Kalamazoo, Michigan
April 2006

ACKNOWLEDGMENTS

I would like to thank Dr. Ho Sung Lee, my thesis advisor, for giving me the opportunity to work on this research work and for his immense support and guidance towards the successful completion of my thesis. I am highly grateful for his technical advice that helped me gain good understanding of my research topic and also for providing me with the required computer facilities to undertake the research.

I would then like to thank my colleagues Mukund Ravindran and Emre Basaran for helping me learn the softwares used in this thesis. Without their technical help and motivation, I could not have completed this project. I take this opportunity to thank my roommates and all my friends for their moral support. I also thank my thesis committee members Dr. Christopher Cho and Dr. Bade Shrestha for showing their interest in my research work.

Finally, I would like to heartily thank my parents and my brother for the affection they show on me and for constantly motivating me towards positivism in life. I thank God, the Almighty for the blessings He has bestowed on me and pray for everybody's happiness.

Bhagavathi Perumal Natarajan

COMPUTATIONAL SIMULATION OF TURBULENT FORCED CONVECTION FLOW OVER A HORIZONTAL PLATE HEATER IN A RECTANGULAR CHANNEL

Bhagavathi Perumal Natarajan, M.S.E.

Western Michigan University, 2006

The phenomenon of turbulent forced convection in the entry region of a rectangular duct was investigated computationally using commercial CFD software, FLUENT. The Standard k-ε turbulence model from FLUENT was used to model turbulence in the 20mm high x 30mm wide cross-sectional rectangular duct. The operating fluid used for the three-dimensional CFD study was water at an inlet temperature of 90°C, with the velocities ranging from 0.5 m/s to 2 m/s, at 1 atm pressure. A constant heat flux was applied to the base of the rectangular channel with the other flow walls insulated. The heat flux ranged from 0 to 20,0000 W/m^2. The effect of different velocities and heat flux values on the heat transfer coefficient and the surface temperature is analyzed. The variation of Nusselt number and wall temperature along the heater surface for different heat fluxes is provided. The thermal boundary layer development for different heat fluxes is also studied using FLUENT. The 3-D numerical results showed good agreement with the available experimental data. A two-dimensional CFD analysis was performed on the given rectangular duct using air as the operating fluid and the correlation to mathematically predict the turbulent forced convection in this 2-D flow geometry is also given.

TABLE OF CONTENTS

Table of Contents—continued

LIST OF TABLES

LIST OF FIGURES

List of Figures—continued

List of Figures—continued

CHAPTER 1

INTRODUCTION

Literature and Scope

The study of forced convective flow in the entry region of rectangular ducts is important in compact heat exchanger applications such as heating and air-conditioning ducts, automobile exhaust systems, radiators and several other heat exchange devices [1, 2]. Analytical solutions for thermally developing flows are available only for simpler situations of ducts with cross sections definable by a single coordinate, such as circular tubes, parallel-plate channels and annular ducts [2, 3]. The case of turbulent flow heat transfer in rectangular ducts requires three-dimensional analysis and is difficult to solve in comparison with the two-dimensional, axi-symmetric analysis of developing flows in circular pipes [4]. The classical analytical methods cannot be easily applied to complex flow problems involving unsteady conditions and complex geometries. Turbulent flows, phase change and chemically reactive flows are some of the fluid flow behaviors, which are still areas of research in theoretical fluid dynamics. Exact solution for turbulent forced convection in rectangular duct is not available due to the non-separable nature of the related eigen value problem [3]. Most of the contributions to the rectangular duct flow problem are purely numerical or approximate approaches.

A relative scarcity of results exists for thermally developing turbulent flow through rectangular ducts leading to less understanding of the flow characteristics of rectangular ducts of interest in engineering applications. This research work deals

with the computational fluid dynamics (CFD) study of single phase, forced convection turbulent flow in rectangular ducts using a commercial CFD software, FLUENT.

Over the past few decades, several works have been conducted in the study of heat transfer in non-circular duct flows, especially rectangular ducts. Aparecido and Cotta [3] analytically studied the thermally developing laminar flow in rectangular ducts by extending the generalized integral transform technique. For laminar forced convection in rectangular ducts with uniform temperature at one or more walls, the Nusselt number was given by Shah and London [2]. Shah and London also provided the Nusselt numbers for fully developed laminar flow in rectangular ducts with uniform wall heat flux at four walls. Fakheri et. al. [5] numerically investigated the hydrodynamically and thermally developing laminar flow in rectangular ducts with conducting walls.

Chandrupatla and Sastri [6] have investigated the laminar forced convection heat transfer of a non-Newtonian fluid in a square duct. Muzychka and Yovanovich [7] developed a new model for predicting Nusselt number for forced convection heat transfer in the combined entry region of non-circular ducts. The model was developed for both fully developed and thermally developing laminar flows in non-circular ducts. Comparisons were made with numerical data for several non-circular ducts and an agreement of within 15 percent was achieved for most duct shapes.

Only a few numerical, experimental and approximate solutions are available for turbulent forced convection through rectangular ducts. Entrance configuration is the key factor affecting flow transition in rectangular ducts [8]. The lower limit of critical Reynolds number along with entrance configuration was investigated by Davies and White [9], Allen and Grunberg [10], Cornish [11] and Hartnett at al. [12].

For fully developed turbulent flow through axi-symmetrically heated rectangular ducts, the friction factor and heat transfer coefficients were given by Rao [13]. Davis and White have provided an experimental study of flow of water in pipes of rectangular section. Turbulent flow in a 1:8 aspect ratio rectangular duct at a Reynolds number of 5800 was investigated both numerically and experimentally by Rokni, Olsson and Sunden [14]. The numerical approach was based on the finite volume technique with a non-staggered grid arrangement and the SIMPLEC algorithm. Direct numerical simulation of turbulent flow and heat transfer in a square duct of low Reynolds number of approximately 4400 was provided by Piller and Nobile [15].

Comparatively, there is less analytical and numerical work found on thermally developing turbulent flows through rectangular ducts, making CFD analysis using FLUENT software ideal for the study of this flow problem. The steady improvement in the speed of computers and the available memory size since the 1950s has led to the emergence of this new third dimension of fluid dynamics, CFD. This branch of fluid dynamics complements experimental and theoretical fluid dynamics by providing an alternative cost effective means of simulating real flows.

Objective of Study

The goal of this project was to develop a FLUENT computational model for turbulent forced convection in a rectangular channel with a flat copper heater at the base. The copper heater creates localized heating at the base of the channel only and rest of the three sides of the rectangular duct is insulated. The turbulent flow in the channel is hydrodynamically fully developed but thermally developing. Commercial CFD software, FLUENT was used to study the fluid flow and temperature distribution in the duct. Conduction within the copper heater and forced convection on the surface

of the heater in contact with the fluid are also analyzed.

Another main purpose of this work was to successfully develop a working FLUENT model of the test section of the flow loop setup of Lee and O'Neill [16, 17]. The test section is the previously mentioned rectangular channel setup with a flat copper heater at the base. The test section was designed by Lee and O'Neill so as to simulate the conditions found in the cylinder head of a 1.6 liter 4 cylinder 16-valve engine previously used in the experiments by Lee and Cholewczynski [18]. The experimental flow loop setup of Lee was found to be representative of conditions found in standard engine cooling systems [19]. Hence, by modeling the experimental flow channel using the FLUENT software, heat transfer in engine cooling could be studied and an accurate mathematical model to predict engine cooling system performance could be developed. Heat transfer in the rectangular channel in the flow loop involves forced convection flow and subcooled flow boiling. In this work, the experimental result obtained from the flow loop of Lee and O'Neill is to be compared with the CFD result obtained from the FLUENT model. However, the effect of subcooled boiling was not included in this FLUENT analysis and only single-phase, turbulent forced convection flow is to be discussed here.

With no accurate mathematical equations available to predict Nusselt number for turbulent forced convection in rectangular ducts, a simplified 2D analysis of the above was performed in FLUENT and the Nusselt number from the CFD results are validated by comparing with the analytical results for turbulent forced convection flow over a flat plate with unheated starting length [20].

CHAPTER 2

GEOMETRY AND NUMERICAL METHOD

Geometry and Computational Domain

The geometry used for the computational analysis of turbulent forced convective heat transfer in rectangular ducts was modeled similar to the test section of Lee and O'Neill [16] as shown in Figure 2.1.

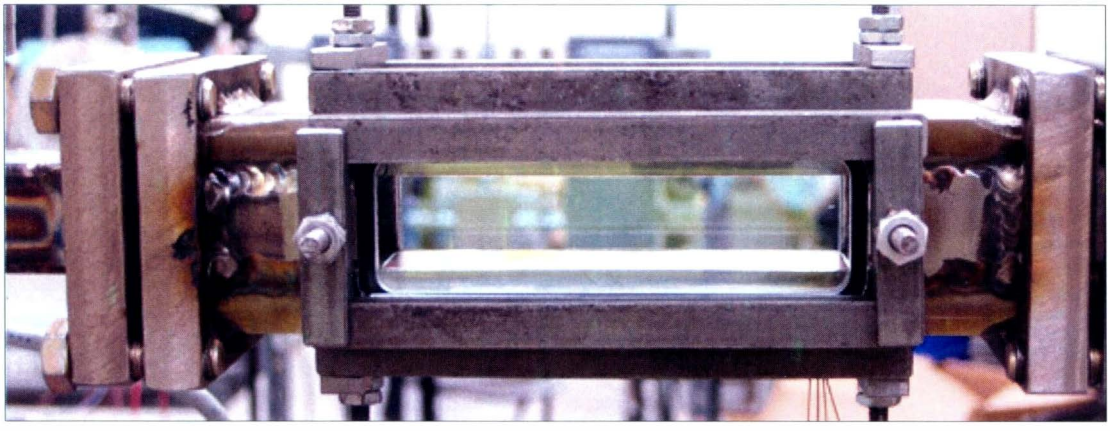

Figure 2.1 Experimental flow loop test section

The computational domain used in this research was modeled using Solidworks [21]. Solidworks is a parametric modeling CAD software in which components are modeled part by part and then the individual parts are assembled together to obtain the final complete geometry. In this work, the computational domain consists of two main components namely, the flow channel and the heater. The assembled flow geometry is shown in Figure 2.2.

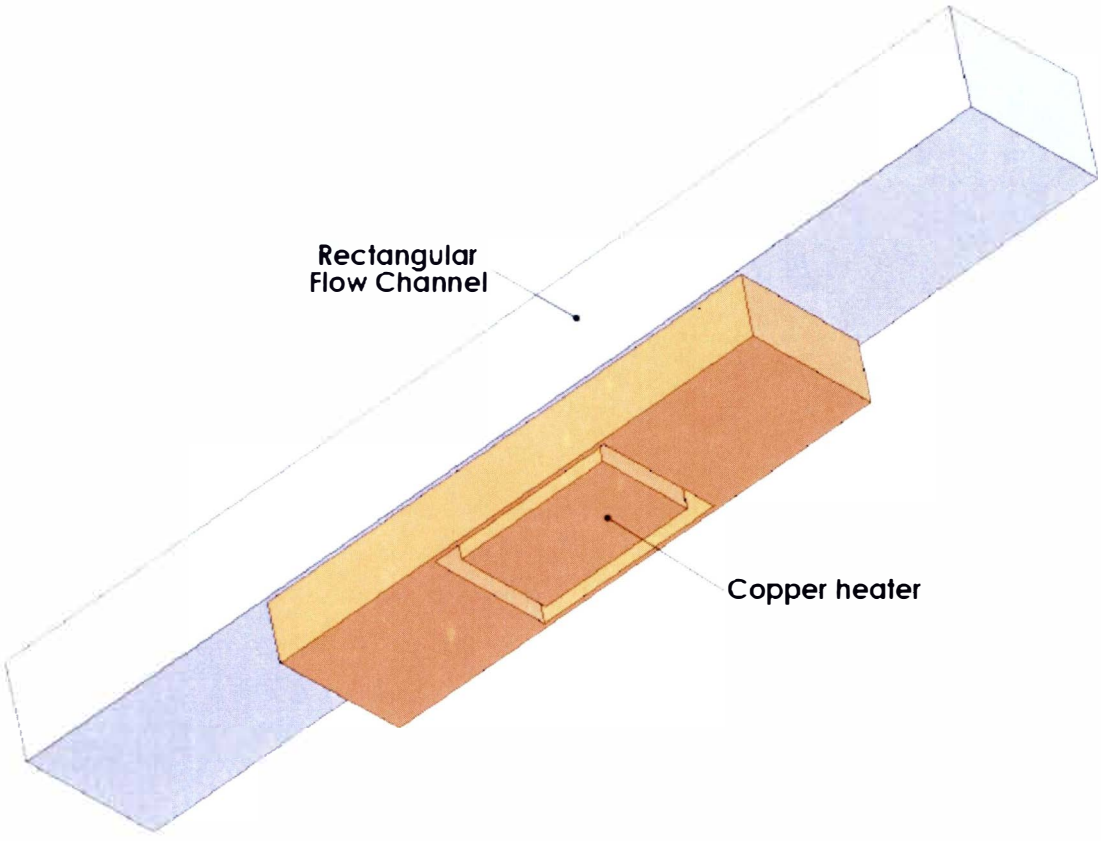

Figure 2.2 Computational domain

Flow Channel

It is a 20mm high x 30mm wide cross-sectional rectangular duct, in which fluid enters through the inlet section at the left and flows over the heater at the bottom and then leaves the test section through the outlet at the right. The heater section forms the base of the flow channel and forced convective heat transfer takes place at the surface of the heater.

Heater Section

The heater section is made of copper and consists of two main components namely the heater and the copper surroundings. The copper heater is a 20mm wide and 30mm long rectangular block of 12mm thickness. A constant heat flux is applied to its base. A 3mm grove separates the copper heater from the copper surroundings and it minimizes the heat leakage from the heater to the surrounding copper. The dimensions of the computational domain are shown in Figure 2.3.

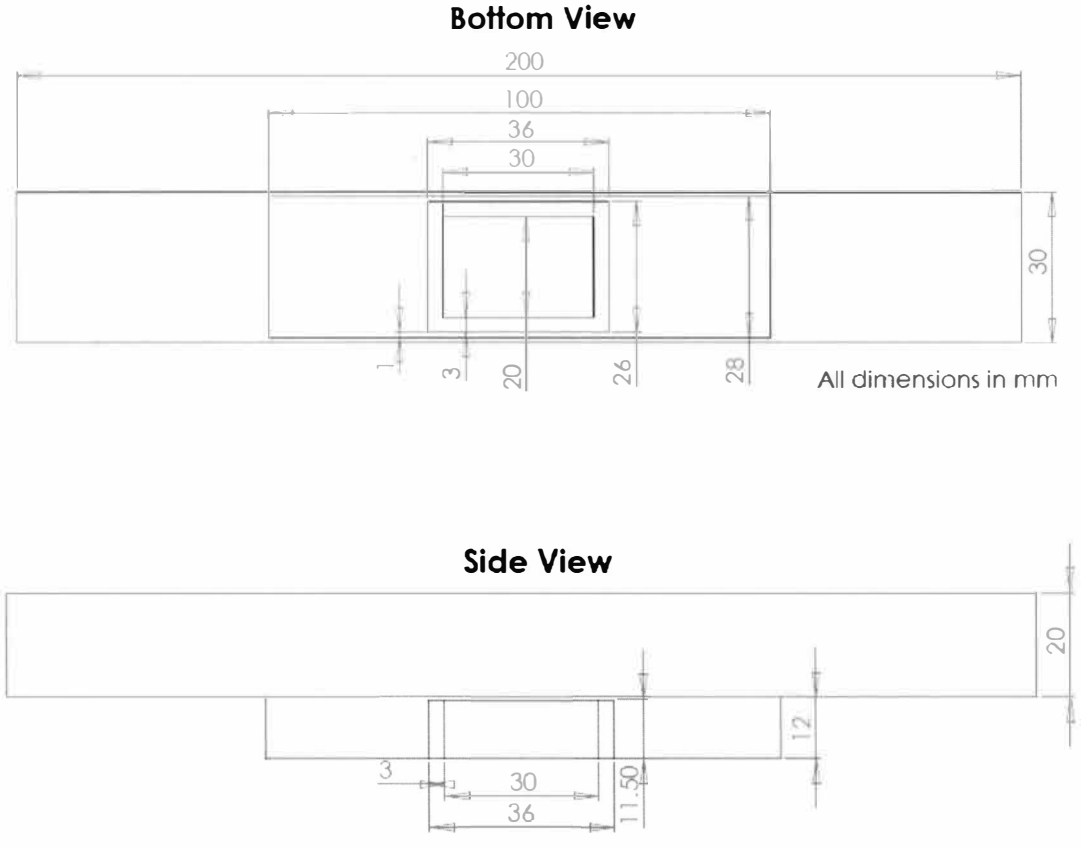

Figure 2.3 Flow channel and heater assembly dimensions

Domain Simplification

The type of physical problem under consideration and the size of the geometry play a key role in CFD analysis. Complexity in the physical problem leads to difficulties in CFD analysis and also increases the uncertainty in the numerically obtained results. For example, the CFD-based predictions are more reliable in laminar flows than in turbulent flows and in single-phase flows more than in multi-phase flows. During CFD pre-processing, the domain or geometry is discretized by means of grid generation and the flow variables are solved only at those finite grid points. It could be imagined that a complex and huge geometry would have millions of grid points in it and the iterative solution process would require large computational speed and memory to obtain numerical solutions. Hence, maximum effort is applied to reduce the size and complexity of the problem when defining the modeling goals in CFD analysis.

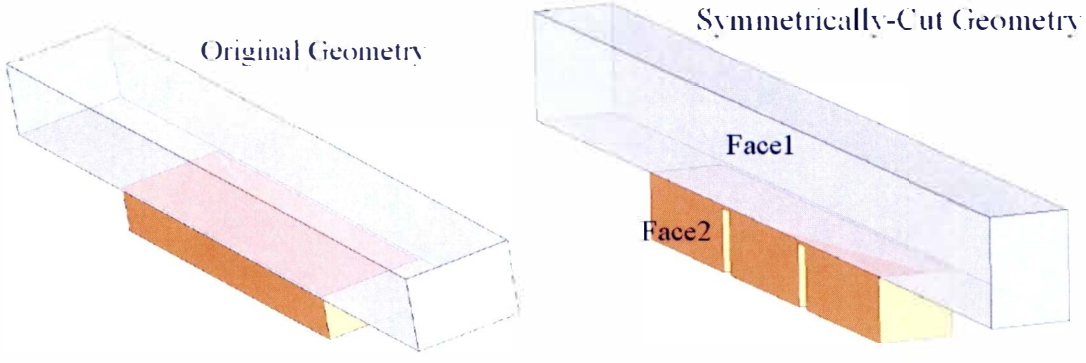

Figure 2.4 Domain simplification

In the given domain, the symmetrically identical feature of the flow channel assembly along the flow axis was made use of to reduce the size of the geometry to be meshed. The flow assembly was symmetrically cut and the size of the physical

problem was reduced to half. Face1 and Face2 shown in Figure 2.4 are the faces generated during the axial-cut and are referred as symmetry planes. FLUENT has capabilities to analyze the symmetrically cut geometry as a complete geometry during the CFD processing.

CFD Theory and Approach

The fundamental equations governing flow of Newtonian, viscous fluid are the continuity and momentum equations. Neglecting body forces, the continuity and momentum equations in rectangular coordinates are given by Equations (2.1) and (2.2). For convenience, the x, y, z coordinates are denoted as x1, x2, x3 and the u, v, w components of velocity as u1, u2, and u3.

$$\frac{\partial \rho}{\partial t} + \frac{\partial}{\partial x_i}(\rho u_i) = 0 \tag{2.1}$$

$$\frac{\partial}{\partial t}(\rho u_i) + \frac{\partial}{\partial x_j}(\rho u_i u_j) = -\frac{\partial p}{\partial x_i} + \frac{\partial}{\partial x_j}\left[\mu\left(\frac{\partial u_i}{\partial x_j} + \frac{\partial u_j}{\partial x_i} - \frac{2}{3}\delta_{i\cdot j}\frac{\partial u_l}{\partial x_l}\right)\right] + \rho g_i \tag{2.2}$$

where i, j = 1,2,3. Equation (2.2) is also known as Navier-Stokes equation. Heat transfer in flow problems is governed by the energy equation given in Equation (2.3).

$$\frac{\partial}{\partial t}(\rho E) + \frac{\partial}{\partial x_i}\left(u_i(\rho E + p)\right) = \frac{\partial}{\partial x_i}\left(k\frac{\partial T}{\partial x_i}\right) \tag{2.3}$$

where E is the total energy. CFD deals with solving these partial differential equations for the given geometry and flow conditions, using a numerical process.

Meshing

In general, the given problem is a continuous domain, in which the flow variables (temperature, pressure or velocity) are defined at every point in the domain. Solving the partial differential equations for flow variables in the continuous domain generates an infinite dimensional problem that cannot be solved by any computers. Hence, in CFD analysis, the given continuous domain is converted into a discrete domain in which the flow variables are defined only at a finite number of grid points. This process of restricting the problem to a finite set of points or cells is called as grid generation or meshing. For instance, in this research, when a heat flux is applied to the base of the heater, heat would be conducted through the thickness of the copper heater. Theoretically, the temperature variation along the center of the heater in the case of a continuous domain would look like Figure 2.5. There would be infinite number of points in a continuous domain and therefore, infinite number of solutions for temperature along the heater center which cannot be solved using computers. For the continuous problem, the temperature, 'T' along the center of the heater is given as:

$$T = T(x), 0 \leq x \leq 12 \text{ mm} \tag{2.4}$$

In CFD pre-processing, the continuous problem domain is replaced with a discrete domain using a grid in which the flow variables are defined only at the grid points. Figure 2.6 shows the computational temperature profile along the center of the discretized copper heater, in which the temperature is defined only at 'N' grid points.

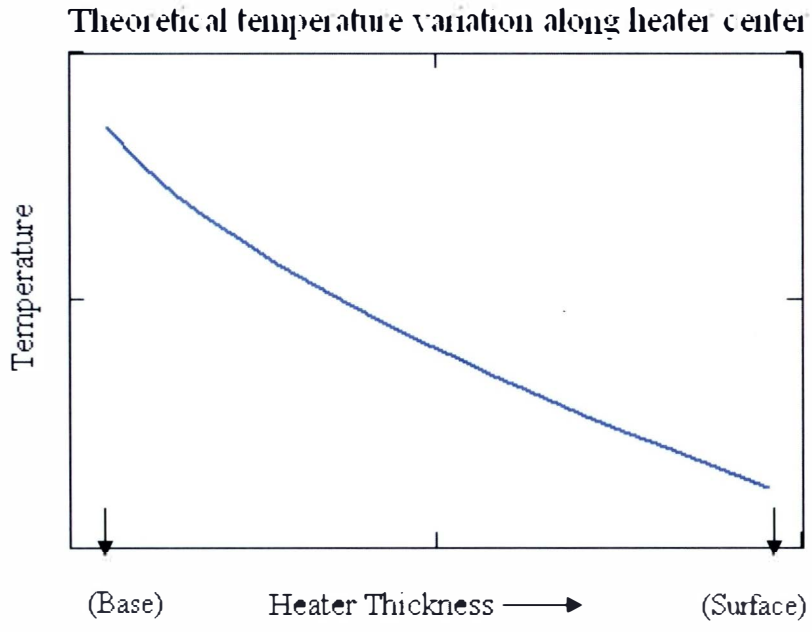

Figure 2.5 Continuous temperature variation curve – Theoretical

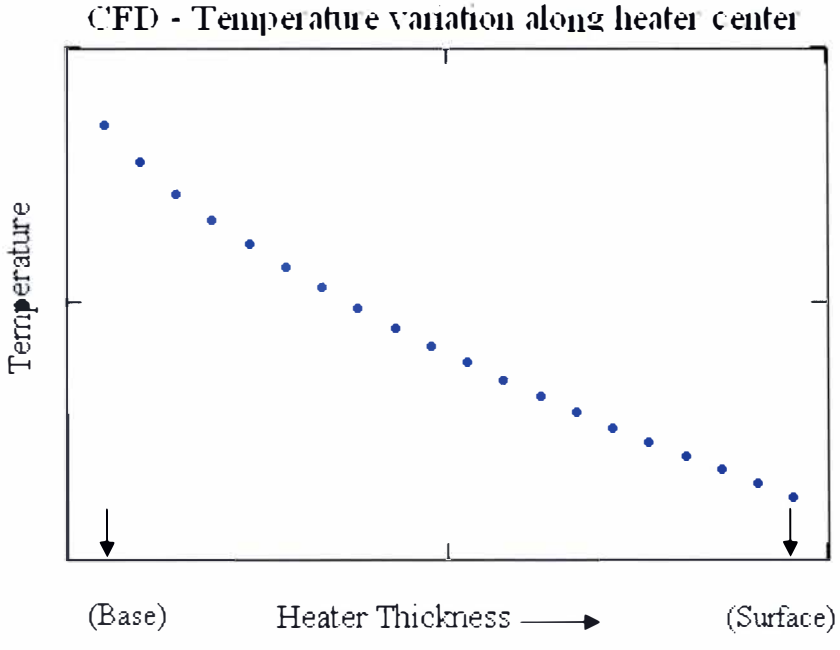

Figure 2.6 Discrete temperature variation curve - CFD

There would be finite number (N) of points in the discrete domain and therefore, finite number of solutions for temperature (N = 20 in Figure 2.6) along the heater center which can be solved using computers. For the discrete problem, temperature 'T' along the center of the heater is given as:

$$T = T(x_i),\ i = 1, 2, \ldots\ldots, N \tag{2.5}$$

Discretization

During meshing, the flow geometry or the continuous domain is sub-divided in to smaller co-domains or control volumes. The governing partial differential equations are then integrated on the individual control volumes to construct algebraic equations for the unknown, discrete dependant variables such as velocity, temperature and pressure. This process is called as discretization and FLUENT uses a control-volume based technique called Finite Volume Method (FVM) to discretize the governing partial differential equations in to discrete, algebraic equations. These discrete, non-linear governing equations are then linearized to produce a system of equations for the dependent variables in every computational cell. The resultant linear system is then solved to yield an updated flow-field solution and the procedure is repeated until convergence is reached.

In this research, the Segregated solver numerical method from FLUENT was used for the above discussed discretization. In Segregated solution algorithm, the governing integral equations for the conservation of mass, momentum, and energy and other scalar such as turbulence are solved sequentially i.e., segregated from one another. Because the governing equations are non-linear and coupled, several iterations of the solution loop must be performed before a converged solution is

obtained. Each iteration in segregated solver solution method consists of the steps illustrated in Figure 2.7 from FLUENT 6.1 User's guide [22].

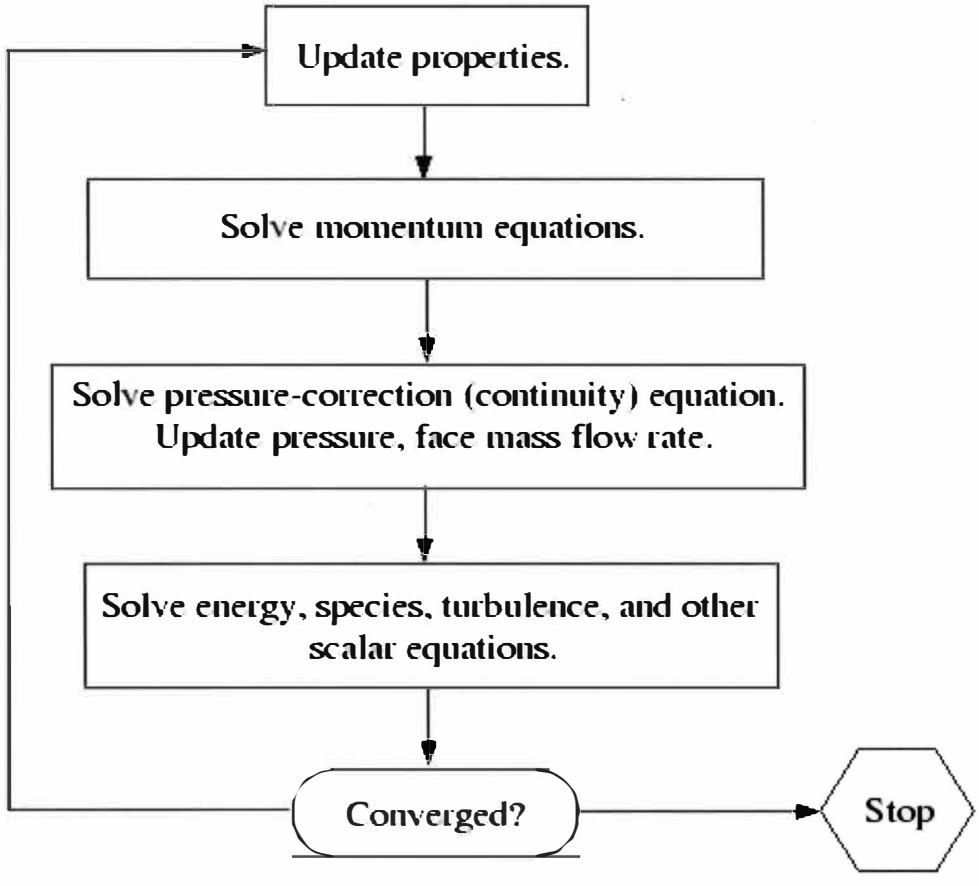

Figure 2.7 Overview of segregated solution method

Since the given problem involves turbulent flow along with heat transfer, the Segregated solver would solve the energy equation and turbulence equation during each iteration in addition to the continuity and momentum equations.

Turbulence Modeling

FLUENT provides two major approaches for modeling turbulence – the

Reynolds-averaged Navier-Stokes (RANS) and Large Eddy Simulation (LES). While the former is well developed and consumes less computational time, the latter is in its infancy stage and requires very large computational time. The Reynolds-averaged approach is generally adopted for practical engineering calculations and it offers many models to simulate turbulence. The RANS Standard k-ε model was used to model turbulence in the rectangular flow channel problem. The Standard k-ε model is one of the simplest and complete turbulent models and had become the workhorse of practical engineering flow calculations since proposed by Launder and Spalding [23]. Robustness, economy, and reasonable accuracy for a wide range of turbulent flows explain its popularity in industrial flow and heat transfer simulations. Standard k-ε model is a semi-empirical model based on model transport equations for the turbulence kinetic energy (k) and its dissipation rate (ε). The model transport equation for 'k' was derived from the exact equation, while the model transport equation for 'ε' was obtained using physical reasoning. The turbulence kinetic energy, 'k', and its rate of dissipation, 'ε', are obtained from the following transport equations [22]:

$$\frac{\partial}{\partial t}(\rho k)+\frac{\partial}{\partial x_i}(\rho k u_i)=\frac{\partial}{\partial x_j}\left[\left(\mu+\frac{\mu_t}{\sigma_k}\right)\frac{\partial k}{\partial x_j}\right]+G_k-G_b-\rho\varepsilon+Y_M+S_k \qquad (2.6)$$

$$\frac{\partial}{\partial t}(\rho \varepsilon)+\frac{\partial}{\partial x_i}(\rho \varepsilon . u_i)=\frac{\partial}{\partial x_j}\left[\left(\mu+\frac{\mu_t}{\sigma_\varepsilon}\right)\frac{\partial \varepsilon}{\partial x_j}\right]+C_{1\varepsilon}\frac{\varepsilon}{k}(G_k+C_{3\varepsilon}G_b)-C_{2\varepsilon}\rho\frac{\varepsilon^2}{k}+S_\varepsilon \qquad (2.7)$$

In Equations (2.6) and (2.7), G_k represents the generation of turbulence kinetic energy due to the mean velocity gradients, G_b is the generation of turbulence kinetic energy due to buoyancy and Y_M represents the contribution of the fluctuating

dilatation in compressible turbulence to the overall dissipation rate. $C_1\varepsilon$, $C_2\varepsilon$, and $C_3\varepsilon$ are constants. σ_k and σ_ε are the turbulent Prandtl numbers for 'k' and 'ε', respectively. S_k and S_ε are user-defined source terms. The calculation of these terms in the Standard 'k' and 'ε' transport equations and the values of the constants are given in FLUENT 6.1 User's guide [22]. Turbulent flows are significantly affected by the presence of walls and hence the enhanced wall treatment method under the standard k - ε turbulence model was activated in FLUENT to get more reasonably accurate simulation results near the walls of the rectangular channel.

CHAPTER 3

THREE DIMENSIONAL CFD ANALYSIS

Computational Mesh

The three-dimensional rectangular flow channel was meshed using GAMBIT meshing software and the volume mesh of the flow setup (half section) is shown in Figure 3.1.

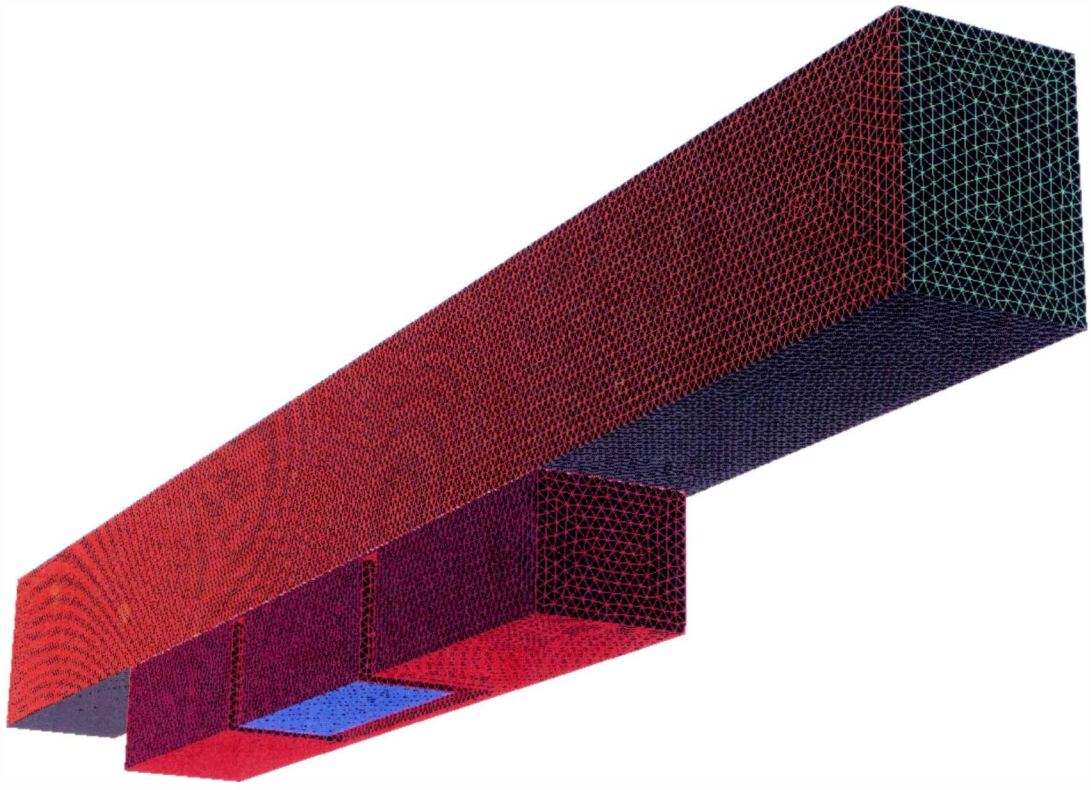

Figure 3.1 3-D Unstructured volume mesh of the flow channel with heater (half section)

An unstructured grid of tetrahedral elements was made use of to mesh the two volumes, rectangular duct and the copper heater. Though tetrahedral meshes generate more mesh points than hexagonal meshes, they are easy to generate for a complex geometry. Finer meshes are often used to get more data points from the flow domain and hence more accurate results. Thus, it is desirable to have denser meshes in the flow domain in order to get more accurate information about temperature and other flow variables. But, finer meshes throughout the given flow geometry would require more computational memory and also longer time to solve.

In the given flow problem, the region around the surface of the heater was the 'most-happening' region in the vicinity of which there was forced convection heat transfer and boundary layer development taking place. There were not any significant changes taking place in other regions of the domain. Hence, it was desired to pack more nodes around the heat surface region and minimal number of grid points in the rest of the geometry. This was achieved in GAMBIT using the Size Function feature [24]. Computational analysis on this discretized domain was carried out using FLUENT.

Boundary Conditions

The turbulent flow simulation is more challenging compared to laminar flows and it is critical to specify realistic boundary conditions in order to get meaningful CFD results.

Velocity Inlet and Turbulent Boundary Conditions

The 'velocity inlet' boundary condition was used to define the flow velocities along with the specification of transported turbulence quantities at the inlet. Using the

k-ε turbulence specification [22], the turbulence quantities - turbulent kinetic energy and turbulent dissipation rate were defined uniform values at the boundary where inflow occurs. In the given hydrodynamically fully developed turbulent flow problem, since the accurate profiles of turbulence quantities were unknown, FLUENT default values of 1 m^2/s^2 and 1 m^2/s^3 were used for turbulent kinetic energy and turbulent dissipation rate respectively. The flow direction and the boundaries involved in the rectangular channel setup are defined in Figure 3.2. The 'velocity inlet' boundary definition panel is given in Appendix A.

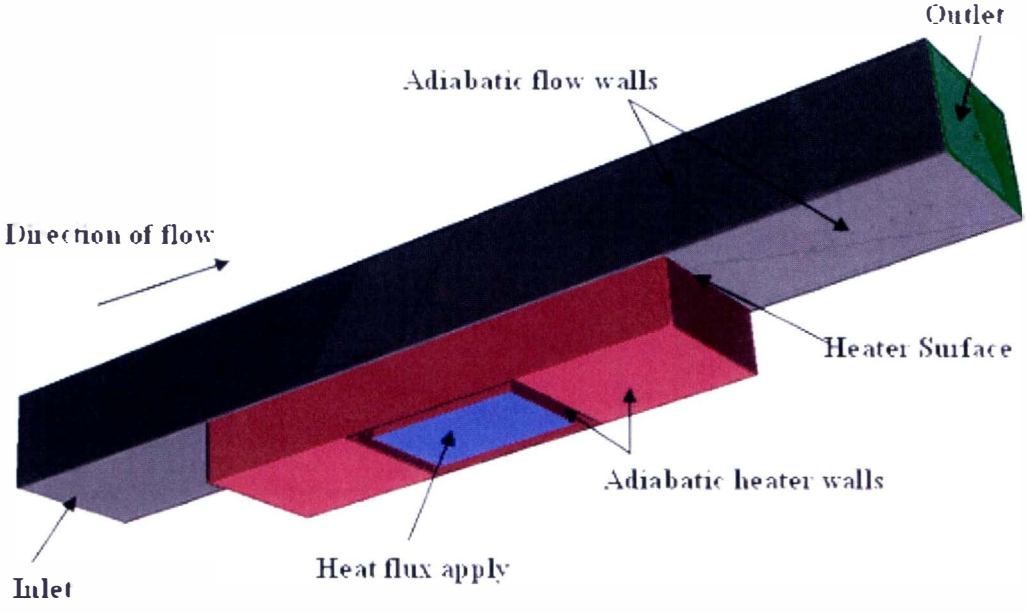

Figure 3.2 Boundary definition in the flow channel and heater assembly

Symmetry Boundary Conditions

Symmetry boundary condition was used in this study because the physical geometry of interest (rectangular flow channel setup) and the pattern of the

flow/thermal solution had mirror symmetry. Face1 and Face2 in Figure 3.3 created during the domain simplification step were defined as symmetrical boundaries. FLUENT assumes zero flux of all quantities across a symmetric boundary. There is no convective flux across a symmetry plane and hence the normal velocity component at the symmetry plane is zero. Also, there is no diffusion flux across a symmetry plane and the normal gradients of all flow variables are thus zero at the symmetry plane. Thus the symmetry boundaries were used to reduce the extent of the computational model to a symmetric subsection of the overall physical system.

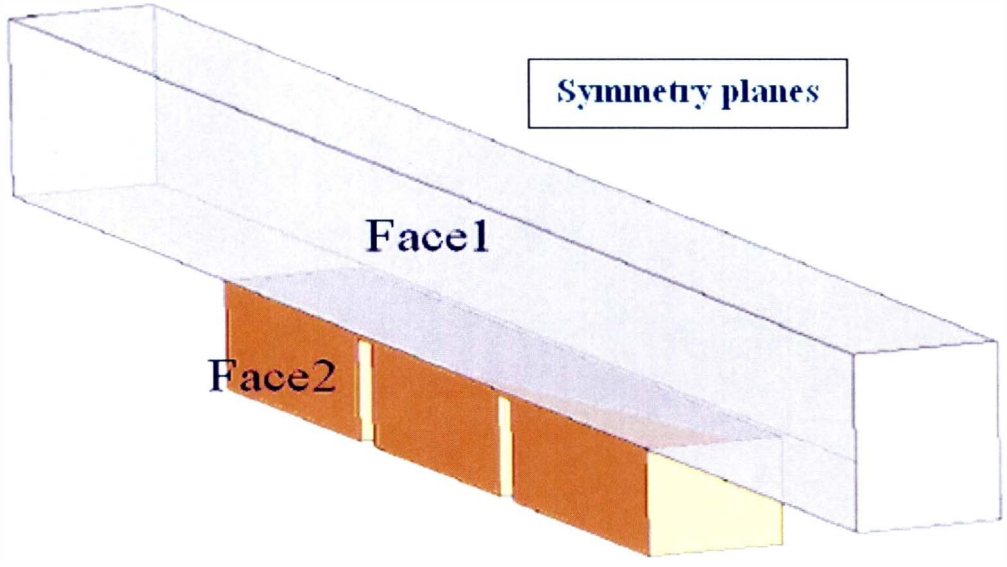

Figure 3.3 Symmetry boundary condition

Thermal Boundary Conditions

In order to solve the energy equation, the thermal boundary conditions at the walls of the heater had to be defined as in Figure 3.2. A uniform heat flux was applied to the base of the copper heater in W/m^2. The heater sidewalls were assigned adiabatic

thermal boundary conditions and hence no heat loss to the atmosphere was assumed. The flow walls in the rectangular duct were also assigned adiabatic conditions. For forced convection to take place, coupled thermal boundary condition was used for the heater surface in contact with the fluid flowing in the rectangular duct. The coupled thermal boundary condition allows heat interaction between the surface of the heater and the bottom plane of the flow channel.

Solution Process

In the solution phase of the given problem, the three conservation equations and the turbulent equations were solved using Segregated solver, second order discretization technique [22] in FLUENT (Refer Figure 2.8). Second order discretization is generally used for complex flow problems to yield more accurate results compared to first order discretization.

Convergence Criteria

In FLUENT, the segregated solver solves the conservation equations sequentially on an iterative basis. At the end of each solver iteration, the residual sum for each of the conserved variables is computed and stored. On a computer with infinite precision, these residuals will go to zero as the solution converges. On an actual computer, the residuals decay to some small value and then stop changing. The solution is converged if all the discretized transport equations are obeyed to a specified tolerance defined by FLUENT residuals and the solution no longer changes with more iteration (Refer Figure 3.4). In FLUENT, the default convergence criterion for all equations is 10^{-3} except the energy equation, for which the criterion is 10^{-6}. In the CFD analysis of the rectangular flow channel, the convergence criteria were set

very low to the order of 10^{-10} and the residuals were monitored until the residual plot decayed to a reasonably small value (lesser than 10^{-6}) and then stopped changing.

Iteration Steps

During the beginning of the iterations, the solution variables were initialized to start computing from the inlet conditions. For the first few hundreds of iterations, the solution was carried out for the laminar flow condition. Once the flow was developed, the turbulent model was activated and the iterations were run until specified convergence tolerance was achieved. This technique of turning on the turbulence model after allowing the flow to develop in laminar conditions yields better results for turbulent flow analysis problems. The residual plot in Figure 3.4 shows the result convergence. All the equations have decayed to the order of below 10^{-6} and the residuals no longer change with more iteration.

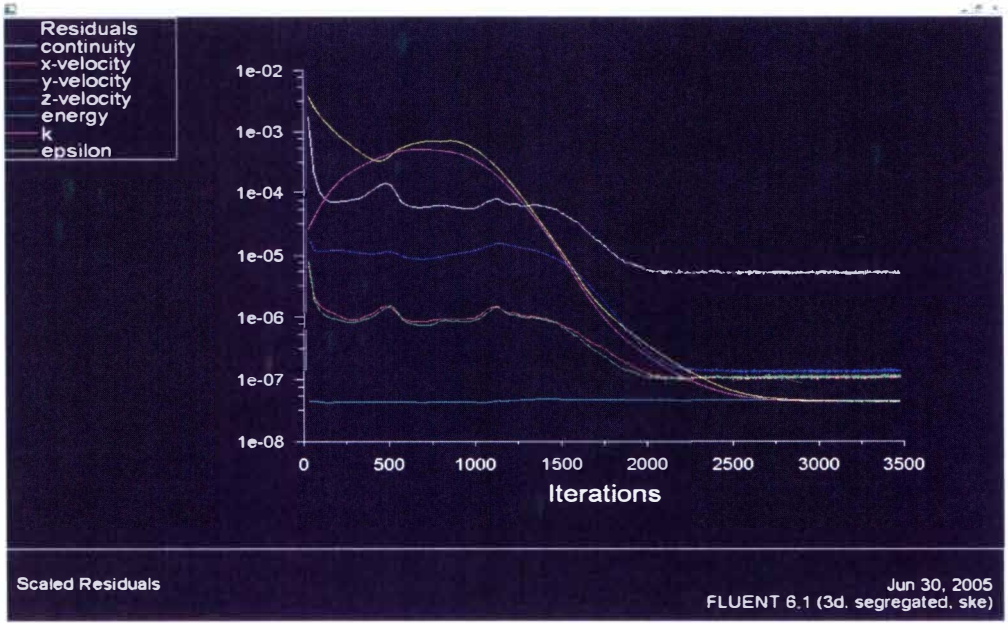

Figure 3.4 Converged residual plot

Validation of CFD Analysis

Validation of results is an important step in the CFD analysis. It is the process of judging how far the CFD model resembles or duplicates the real situation. In this research work, the computational domain was modeled exactly similar to the test section in the experimental flow loop setup of Lee and O'Neill [17]. Hence, the CFD simulation results from FLUENT were validated by comparing with the experimental data from the flowloop setup of O'Neill.

Comparison of CFD and experimental results

Lee and O'Neill conducted experiments for different inlet temperatures and velocities of water and recorded the temperature distribution along the 12 mm thick copper heater for varying heat fluxes. In order to measure the temperature distribution along the copper heater, four thermocouples (T1, T2, T3 and T4) were incorporated at the center of the heater as shown in Figure 3.5 [18].

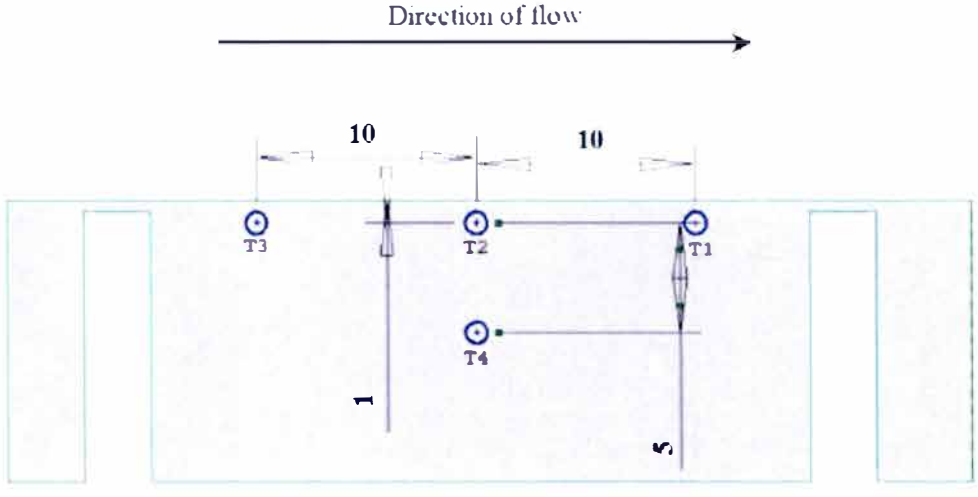

Figure 3.5 Four thermocouples at the center of the heater – Experimental arrangement

The measured heat flux between the thermocouple points T2 and T4 from experimentation was applied to the heater base in the CFD analysis. Using the Surface-Point function [22] in FLUENT, temperatures at the four locations in the copper heater for different heat fluxes were calculated and were successfully compared with the experimental thermocouple temperatures as shown in Figure 3.6, Figure 3.7, Figure 3.8 and Figure 3.9. Comparisons of FLUENT and experimentation results shown below are for conditions in which water enters at 90 °C at an inlet velocity of 1 m/s at 1 atmospheric pressure. The heat flux applied to the base of the copper heater ranged from 0 to 400000 W/m^2. The CFD results from FLUENT compared well with the experimental results for different heat flux values. A good agreement between the CFD results and experimentation data proved that the single-phase 3-D CFD model used to simulate turbulent forced convection in a rectangular duct with flat heater was accurate.

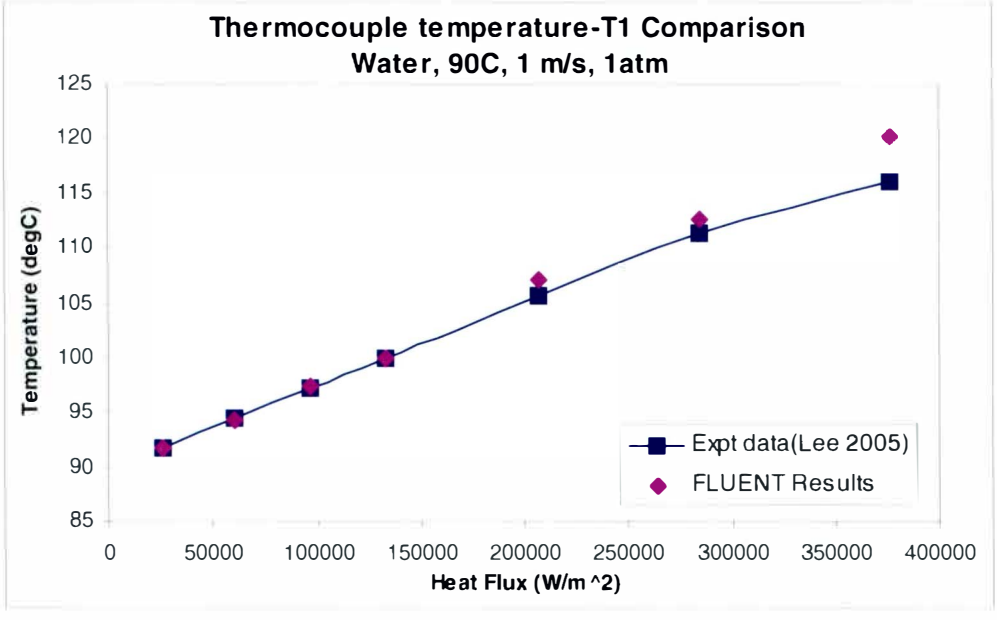

Figure 3.6 Comparison of experimental thermocouple data (T1) with CFD results

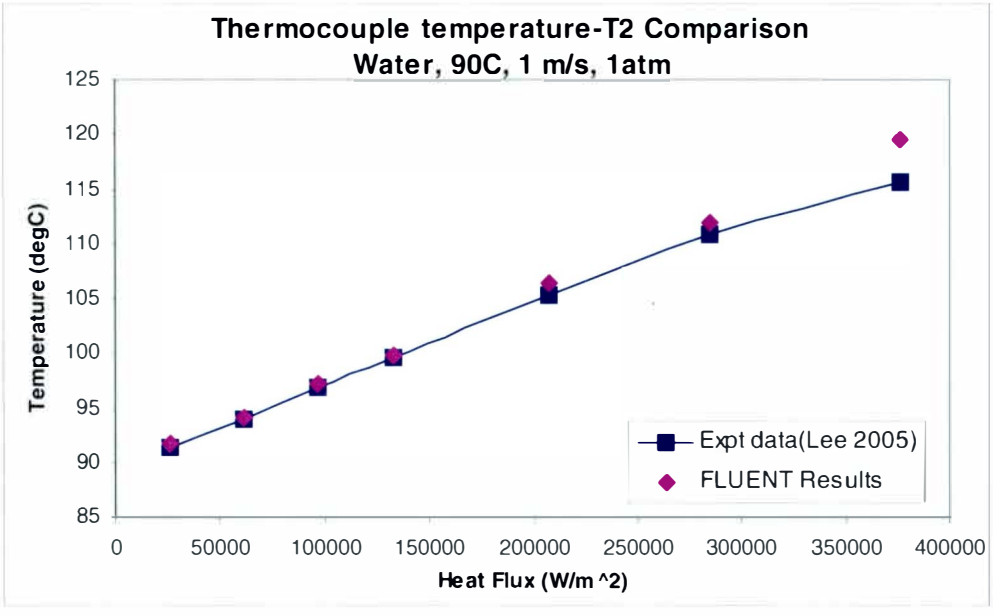

Figure 3.7 Comparison of experimental thermocouple data (T2) with CFD results

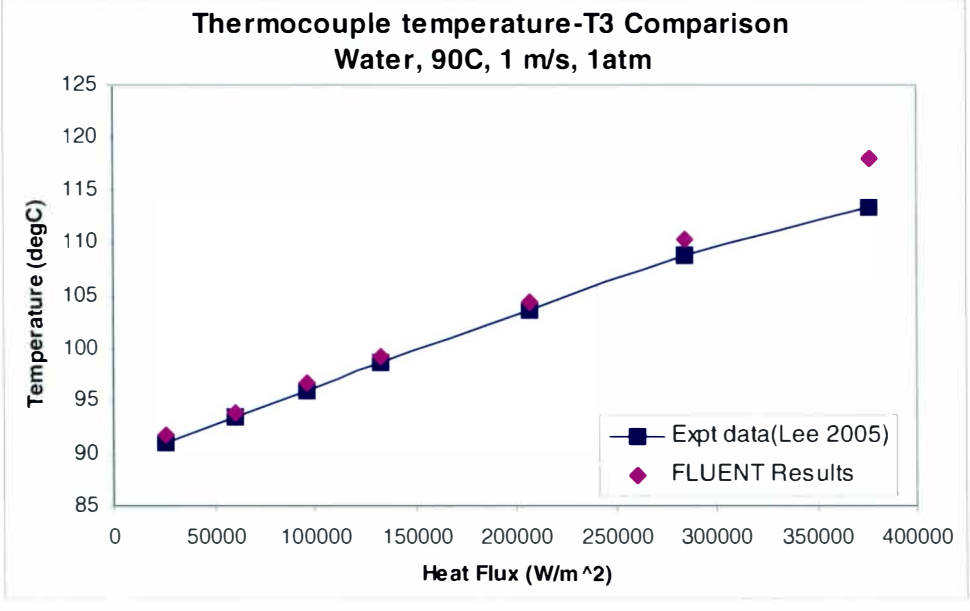

Figure 3.8 Comparison of experimental thermocouple data (T3) with CFD results

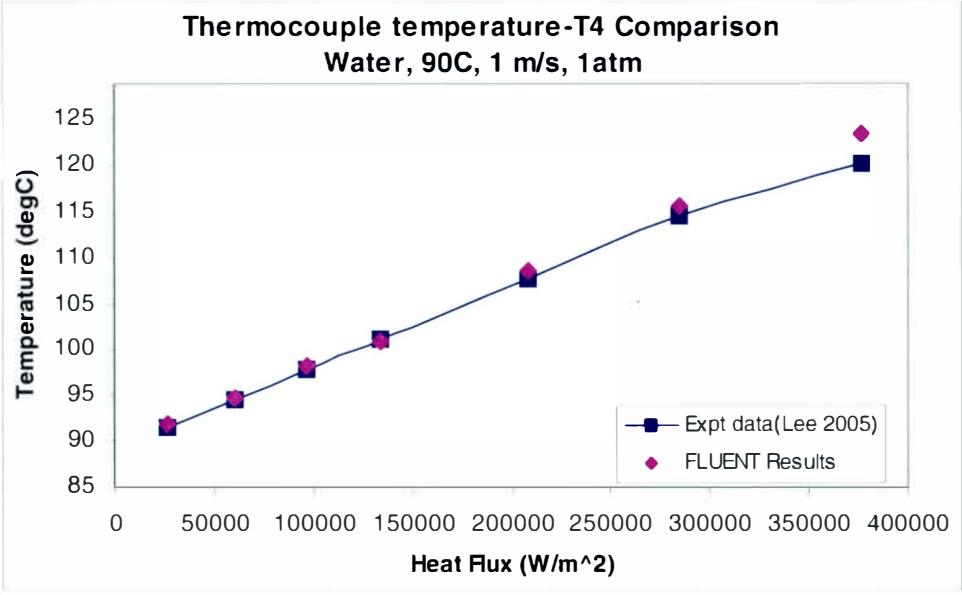

Figure 3.9 Comparison of experimental thermocouple data (T4) with CFD results

For higher heat fluxes (above 250,000 W/m^2), the computational thermocouple temperature results starts to deviate because of boiling heat transfer in the experimental flow loop test section.

Mesh Independence

Successful computation of turbulent flows greatly depends on the mesh generation and the computational results can be called accurate only when they do not change significantly when the mesh changes (refinement and coarsening). In order to assess the effect of the number of mesh points on the accuracy of the CFD results, grid independence study was conducted on the rectangular channel domain using three different types of meshes – coarse, medium and fine grids as given in Table 3.1. A very fine mesh and a coarse mesh were generated for the rectangular flow channel geometry and the CFD results obtained from them were compared with that of

standard mesh (200 x 20 x 30). Figure 3.10 shows the comparison of the temperature drop along the center of the 12mm thick copper heater for the coarse, standard and fine meshes. The temperature drop data obtained from FLUENT were for inlet conditions of 1 m/s velocity of water at 90°C inlet temperature when 60,650 W/m^2 heat flux was applied to the heater base.

Table 3.1

Grid independence study using coarse, medium and fine meshes

Mesh	Grid Points	Tetrahedral Cells
Coarse mesh	130 x 20 x 13	133630
Standard mesh	200 x 30 x 20	464490
Fine mesh	400 x 60 x 40	971630

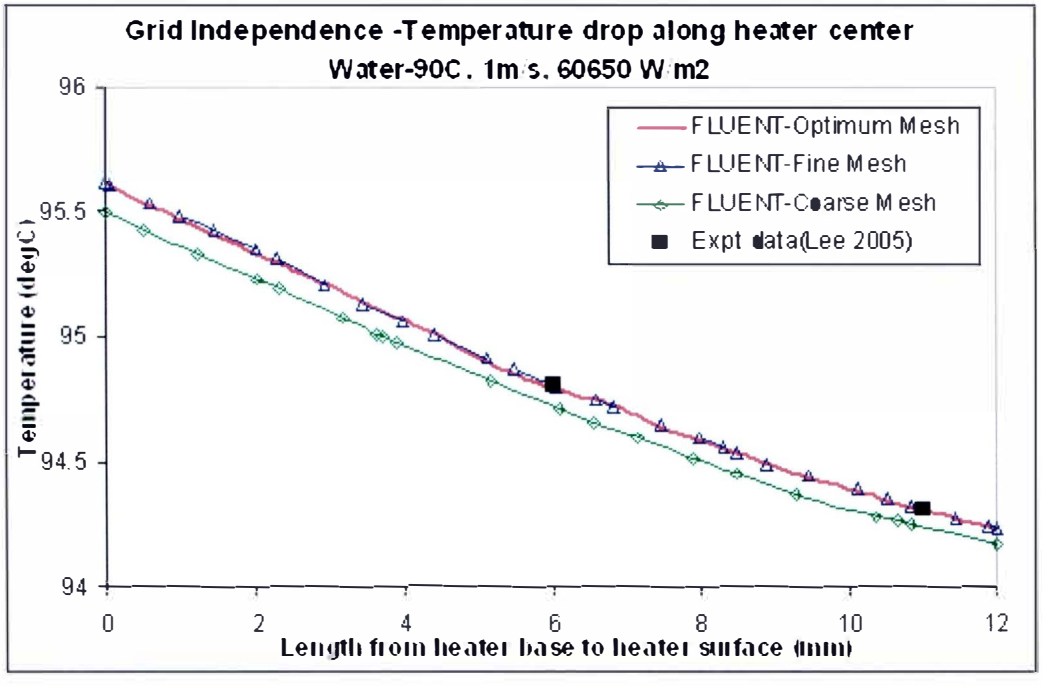

Figure 3.10 Grid independence study– Temperature drop along heater center

Good agreement between the standard mesh and the fine mesh data indicated that the simulation results did not change when the mesh density was increased and thus verified the accuracy of the CFD results. The very coarse mesh yielded slightly offset and incorrect temperature results as expected.

This grid independency analysis showed that the standard mesh (200 x 30 x 20) was the optimum mesh for the CFD analysis of the rectangular channel flow setup and also verified the correctness of the mesh used in this study.

CHAPTER 4

TWO DIMENSIONAL CFD ANALYSIS

In this chapter, a two-dimensional computational analysis of the rectangular flow channel was carried out using FLUENT to better understand the heat transfer taking place within the copper heater and to analyze the boundary layer development over the heater surface. Based on the 2-D computational results obtained, the best empirical correlation to predict 2-D turbulent forced convection in the experimental setup of Lee and O'Neill was found. A 2-D CFD study of laminar forced convection flow in the rectangular duct was also performed.

Problem Description and 2-D Numerical Analysis

A simplified, two-dimensional geometry of the rectangular flow channel setup to be studied is shown in Figure 4.1. The 2D geometry is exactly similar to the cross-sectional view of the original 3-D geometry along the axis.

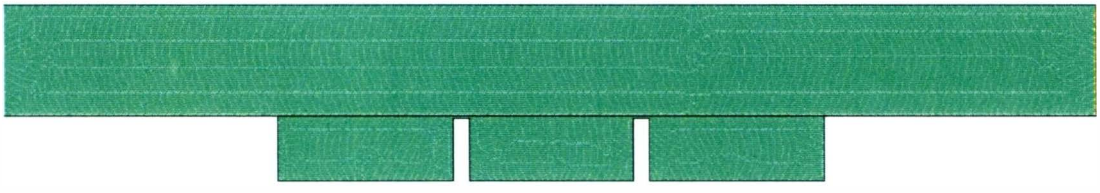

Figure 4.1 Two-dimensional geometry of flow loop test section

In this CFD analysis, all fluid properties were assumed to be constant and the flow to be hydrodynamically developed turbulent flow. The direction of fluid flow

was from left to right. A constant heat flux was applied to the base of the copper heater, which leads to the development of a thermal boundary layer on the surface of the heater. The sidewalls of the heater were assumed to be adiabatic and heat loss from the copper heater to the surrounding air through natural convection was neglected.

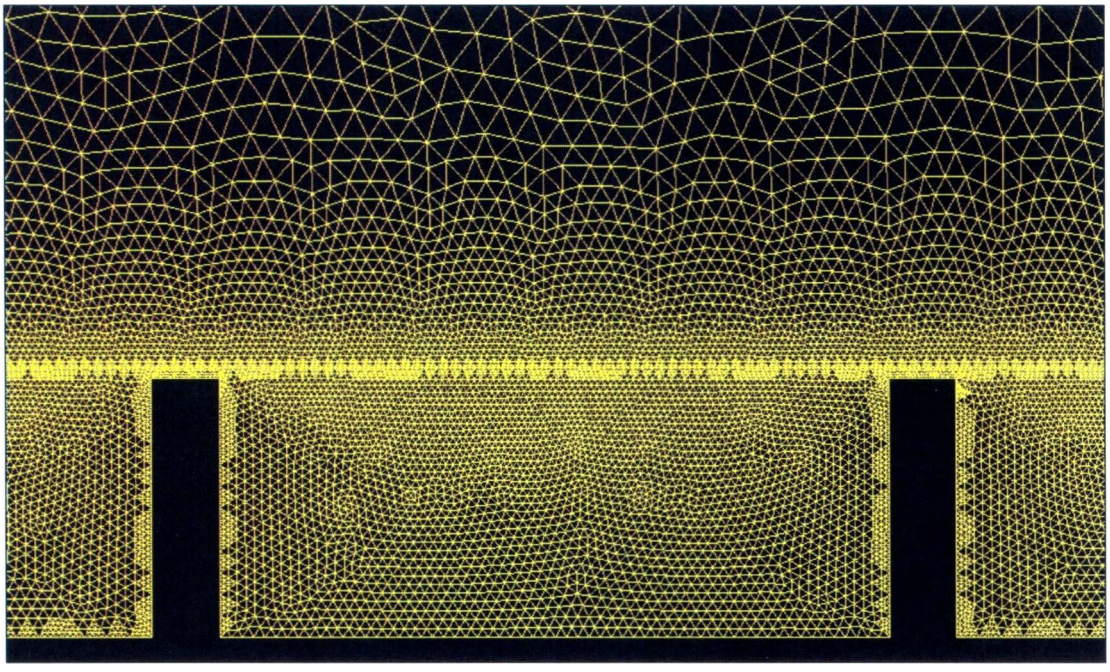

Figure 4.2 Fine 2-D unstructured triangular face mesh - grid adaptation (not to scale)

An unstructured 2-D mesh was generated for the flow geometry using triangular elements in GAMBIT meshing software. While meshing the 2-D domain, utmost care was taken to generate a fine mesh near the heater walls in order to capture the boundary layer and temperature gradient around the heater surface. Grid optimization techniques such as 'Sizing function' [24] in GAMBIT and 'Grid adaptation' technique [22] in FLUENT were employed to generate a fine grid in the

copper heater region where there was large variation in temperature and other properties taking place. The mesh density was gradually reduced along the flow channel since there was not any significant change in fluid properties occurring away from the heater. A close-up view of the mesh density around the copper heater region is shown in Figure 4.2. This mesh optimization technique highly enhances the CFD processing speed with the available computational memory.

The CFD solution process was carried out using the segregated solver - second order discretization technique and turbulence was modeled using the Standard k-ε turbulence equation. For an inlet velocity of 1 m/s of water at 90°C inlet temperature and 1 atm pressure, contours of temperature obtained from FLUENT is shown in Figure 4.3. The heat flux applied to the base of the heater was 60650 W/m^2.

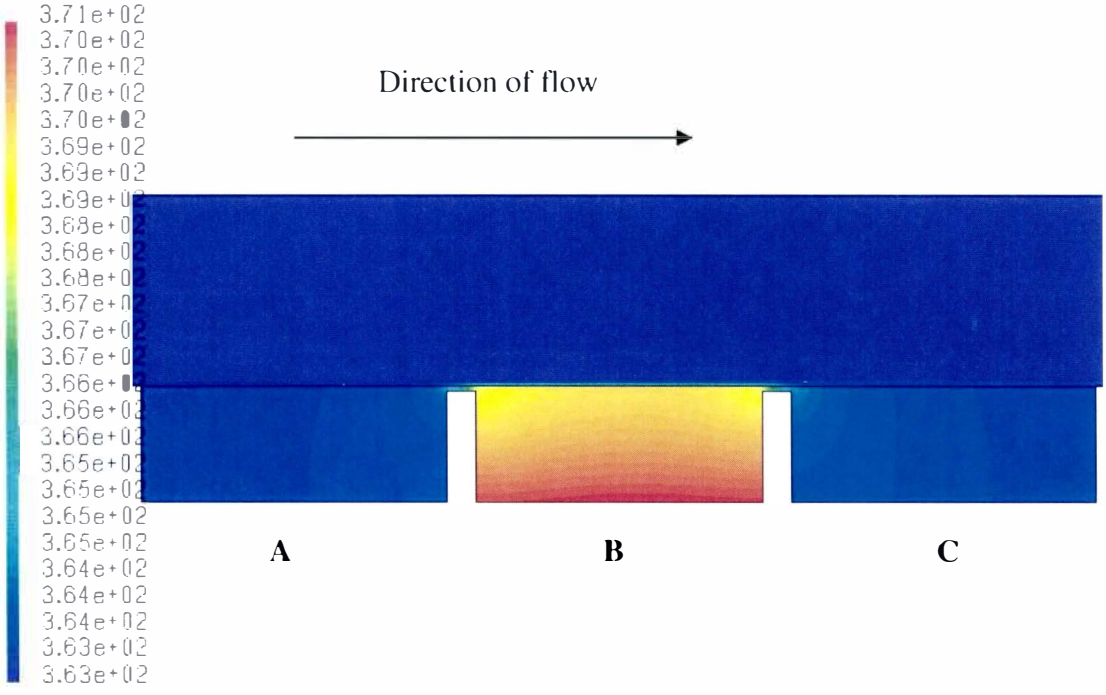

Figure 4.3 Temperature distribution around copper heater- Water at 90°C, 1m/s velocity, 60650 W/m^2 heat flux (Sections A and C are the copper surroundings, B is the copper heater)

The temperature plot from FLUENT indicates that there is significant heat leakage to the copper surroundings (A and C) through the 0.5mm thick copper layer beneath the heater surface on both the sides of the copper heater (B). Though sections A and C of the copper heater are geometrically symmetrical, the forced convection heat transfer taking place on their surfaces is not identical. The difference in temperature between section A of the heater and the fluid is higher than that of the temperature difference between section C and the fluid. This leads to more heat transfer at section A of the copper surrounding than section B. It is also noted that the thermal boundary layer thickness (δ_T) over the heater surface is very thin and change in the temperature of the fluid is taking place only at the vicinity of the heater surface. The fluid temperature remains almost constant elsewhere.

Table 4.1

Comparison of thermocouple data: 2-D and 3-D computational analysis

Thermocouple Temperature Data Comparison - Water at 90°C, 1 m/s				
Heat flux (W/m^2)	**Thermocouple**	**Experimental data (°C)**	**FLUENT Data (°C)**	
			3-D Analysis	**2-D Analysis**
60650 W/m^2	**T1**	94.42	94.31	96.41
	T2	94.04	94.18	96.15
	T3	93.51	93.91	96.02
	T4	94.69	94.81	96.91

A comparison between the thermocouple temperature data obtained from 3-D and 2-D computational analysis for water at 90°C, 1 m/s velocity at 60650 W/m^2 heat

flux is shown in Table 4.1. The temperature of thermocouple T3 is lesser than that of T1 as expected in both the CFD analysis. Also, the thermocouple temperatures of 3-D computational analysis are less than that of the thermocouple data of 2-D CFD simulation. This is because in 3-D simulation, there is more heat leakage to the copper surroundings when compared to the 2-D geometry. This heat loss in turn reduces the overall thermocouple temperatures in 3-D computation.

2-D Mathematical Analysis – Turbulent Forced Convection

Nusselt Number Correlation

For turbulent forced convection at high velocities, the thickness of the thermal boundary layer (δ_T) developed would be very small. In this work, the thermal boundary layer for water flowing over the heater surface at 90°C, 1 m/s velocity, at a heat flux of 60650 W/m^2 was very thin as shown in Figure 4.3. For higher inlet velocities of water at 2 m/s or 3 m/s, the thermal boundary layer thickness was even thinner compared to the overall height of the rectangular duct. Thus, in the two-dimensional analysis of the rectangular flow channel, the boundary layer develops freely, without any constraint imposed by the top wall of the 2-D flow geometry. But, this flow condition is analogous to that of external forced convective flow. Hence, a reasonably good assumption can be made that the 2-D turbulent forced convective flow through the flow geometry used in this research is similar to that of turbulent forced convection over a flat plate with unheated starting length. The 2-D mathematical analysis of the flow loop test section was performed based on this assumption. The simplified 2D duct geometry used to compare with the flat plate heat transfer mechanism is shown in Figure 4.4.

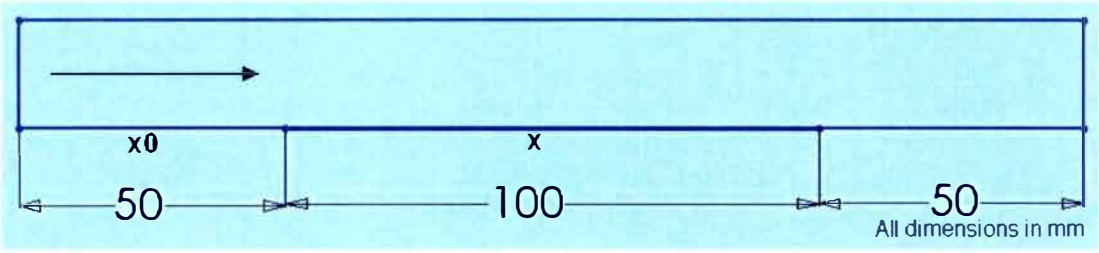

Figure 4.4 Two-dimensional duct with unheated starting length (x0)

The empirical correlation for the local coefficient of friction ($C_{f,x}$) for turbulent forced convection on a flat plate (x0 = 0) was given by Schlichting [25] as in Equation (4.1). Re_x is the local Reynolds number.

$$C_{f,x} = 0.0592 \cdot Re_x^{-1/5} \qquad Re_x < 10^7 \tag{4.1}$$

Using Equation (4.1) with Chilton-Colburn analogy equations [26, 27], the local Nusselt number for turbulent forced convection on a flat plate was found as [28]:

$$Nu_x = 0.0296 \cdot Re_x^{4/5} \cdot Pr^{1/3} \qquad 0.6 < Pr < 60,\ x0 = 0 \tag{4.2}$$

where, Pr is the Prandl Number. The above Nusselt number equation is for turbulent flow on a fully heated flat plate with x0 = 0. In case of a flat plate with unheated starting length (x0 ≠ zero), a correction factor has to be introduced to take into account the discontinuity in wall temperature. A semi-empirical integral analysis was carried out by Reynolds et al. [29] for turbulent boundary layer on a flat plate with unheated starting length (x0) and the correction factor to be multiplied with the local coefficients to include the effect of 'x0' was given as [30]:

$$\left[1-\left(\frac{x_0}{x}\right)^{\frac{9}{10}}\right]^{-\left(\frac{1}{9}\right)} \tag{4.3}$$

where, x0 is the unheated starting length and x is the length of the heating surface. The Nusselt number for turbulent forced convection flow on a flat plate with unheated starting length (x0) was obtained by combining Equations (4.2) and (4.3) as shown in Equation (4.4) [31]. This equation is now suitable for the mathematical analysis of the 2-D flow loop test section.

$$\boxed{Nu_x = \frac{0.0296 \cdot \mathrm{Re}_x^{4/5} \cdot \mathrm{Pr}^{1/3}}{[1-(x_0/x)^{9/10}]^{1/9}}} \tag{4.4}$$

Local Nusselt Number Comparison – Computational vs Analytical solution

Consider air flowing through the simplified 2-D geometry of the flowloop test section shown in Figure 4.4 at an inlet temperature of 353 K and high inlet velocity of 10 m/s. The temperature distribution along the heater surface at a heat flux of 400 W/m^2 was obtained from FLUENT and is shown in Figure 4.5.

In the 2-D CFD analysis, based on the heater wall temperatures (T_w) obtained from FLUENT, the local heat transfer coefficient (h_x) can be calculated as below:

$$h_x = \frac{q''}{T_w - T_f} \tag{4.5}$$

where, q'' is the known constant heat flux applied to the heater surface and T_f is the bulk fluid temperature (Here, T_f = 353 K).

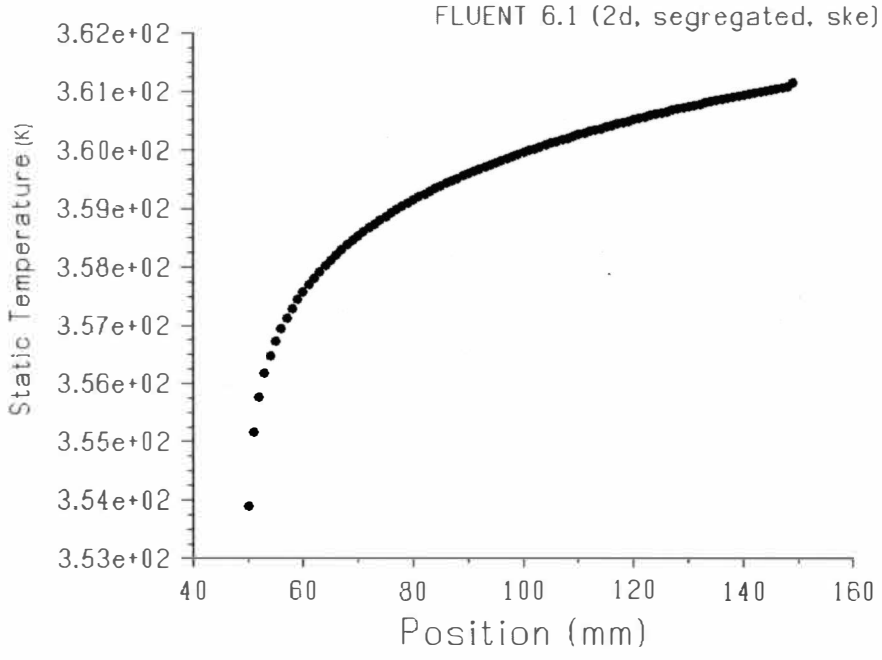

Figure 4.5 Temperature distribution along the heater surface for 400 W/m^2 heat flux

Then the local Nusselt number (Nu_x) for turbulent flow through the 2-D rectangular flow channel can be obtained computationally using the standard Nusselt number Equation (4.6).

$$Nu_x = \frac{h_x \cdot x}{k} \tag{4.6}$$

where, 'x' is the length of the heating side and 'k' is the thermal conductivity of the fluid. The local Nusselt number at the surface of the heating side (x = 51mm to 150mm) for different inlet velocities of air (10 m/s, 12.5 m/s and 15 m/s at 353 K inlet temperature) at a heat flux of 400 W/m2 is shown in Figure 4.6. It was noted that the Nusselt number values increased with increase in inlet velocities.

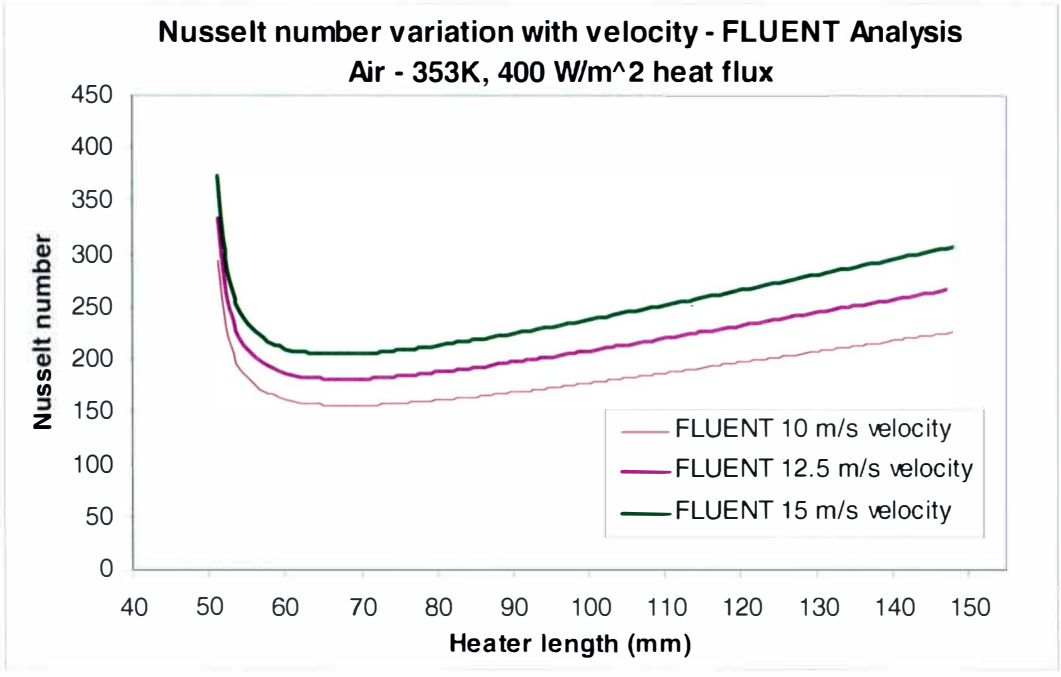

Figure 4.6 Local Nusselt number profile for different velocities – CFD analysis of air at 353 K for 400 W/m^2 heat flux

The successful comparison between 2-D computational Nusselt number solutions and the analytical results obtained from Equation (4.9) is given in Figure 4.7 and Figure 4.8. The Nu_x values are for air at 353K entering at inlet velocities of 10 m/s and 15 m/s respectively and the heater surface is subjected to a constant heat flux of 400 W/m^2.

Overall, the CFD and analytical Nusselt number results compared well and the error between these two results was less than 10%. This verified that for turbulent flows, the single-phase heat transfer taking place in the 2-D rectangular test section was similar to that of turbulent forced convection on a flat plate with unheated starting length (x0).

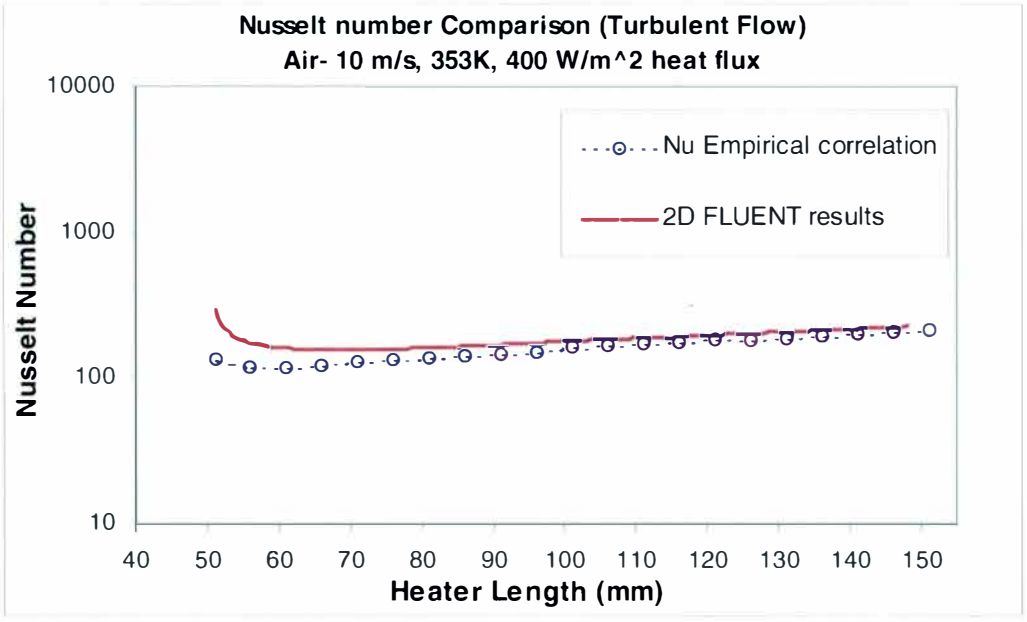

Figure 4.7 Nusselt number Comparison – CFD vs Eqn (4.4) results, Air 10 m/s, 353K, 400 W/m^2 heat flux (log scale) – Turbulent flow

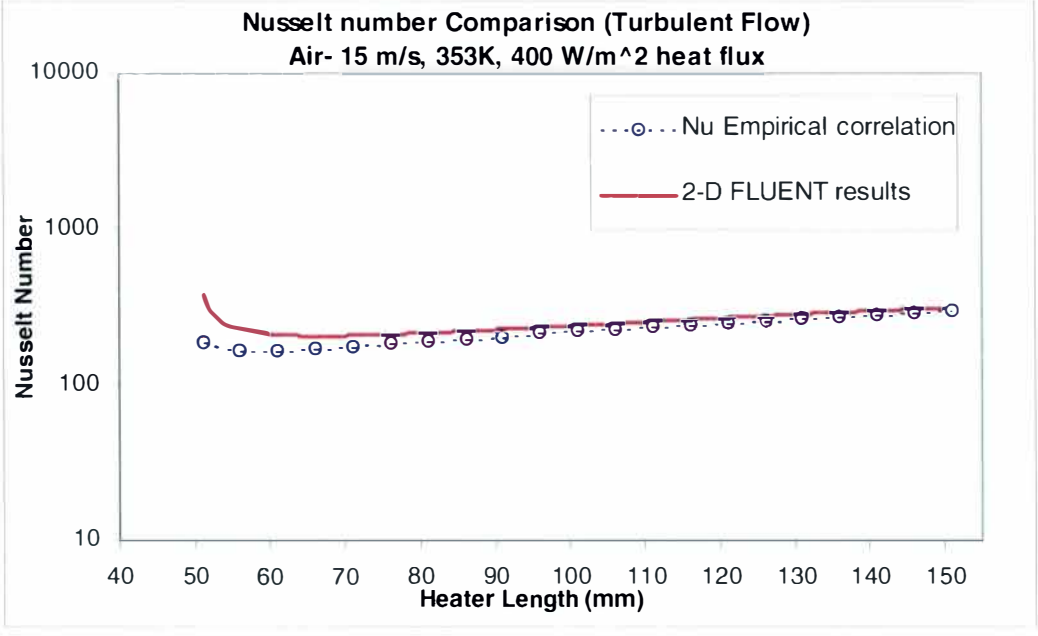

Figure 4.8 Nusselt number Comparison – CFD vs Eqn (4.4) results, Air 15 m/s, 353K, 400 W/m^2 heat flux (log scale) - Turbulent flow

Boundary Layer

The velocity boundary layer thickness (δ) for the flat plate turbulent flow problem is given by Equation (4.7) [32].

$$\delta = 0.37 \cdot x \cdot \mathrm{Re}_x^{-1/5} \tag{4.7}$$

For turbulent flows, the boundary layer growth does not depend on the Prandl number and is mainly influenced by random fluctuations in the fluid [33]. Hence, Equation (4.7) can also be used to obtain the thermal boundary layer thickness (δ_T).

For turbulent flows, $\delta \approx \delta_T$ (4.8)

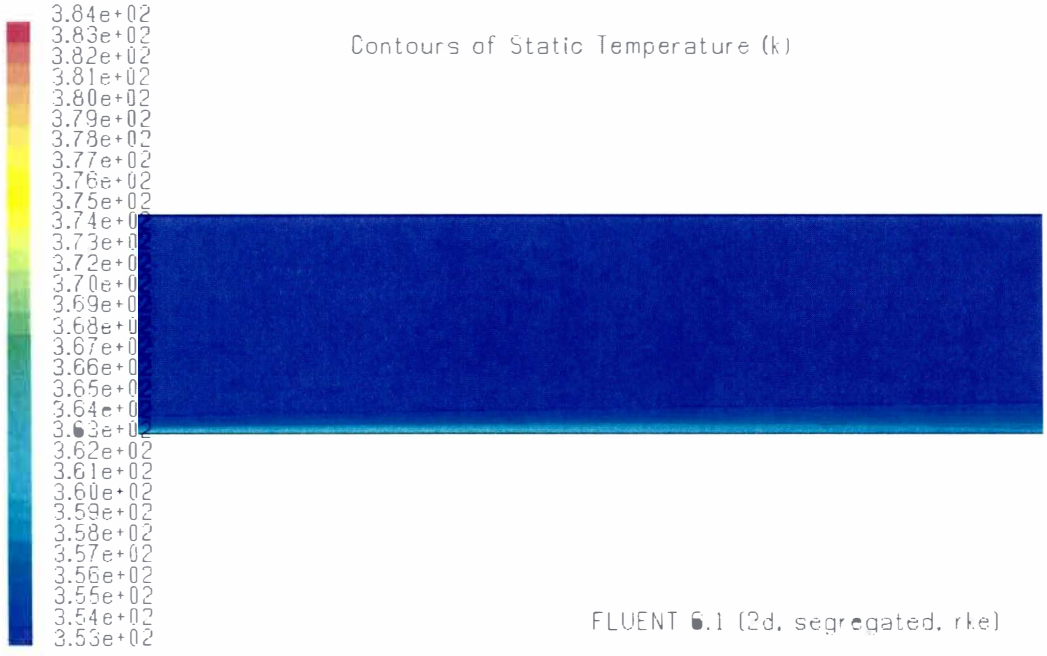

Figure 4.9 Thermal boundary layer for air at 353 K, 10m/s velocity, 400 W/m^2 heat flux

Consider air at an inlet temperature of 353 K to flow through the 2-D geometry of the flowloop test section shown in Figure 4.4 at a high velocity of 10 m/s. The thermal boundary layer developed when applying a heat flux of 400 W/m^2 to the heater surface (x = 51 mm to 150 mm) is shown in Figure 4.9. The boundary layer thickness can also be studied mathematically using the Equation (4.7). Figure 4.10 shows the theoretical boundary layer development at 10 m/s, 15 m/s and 20 m/s velocities for air at 353 K.

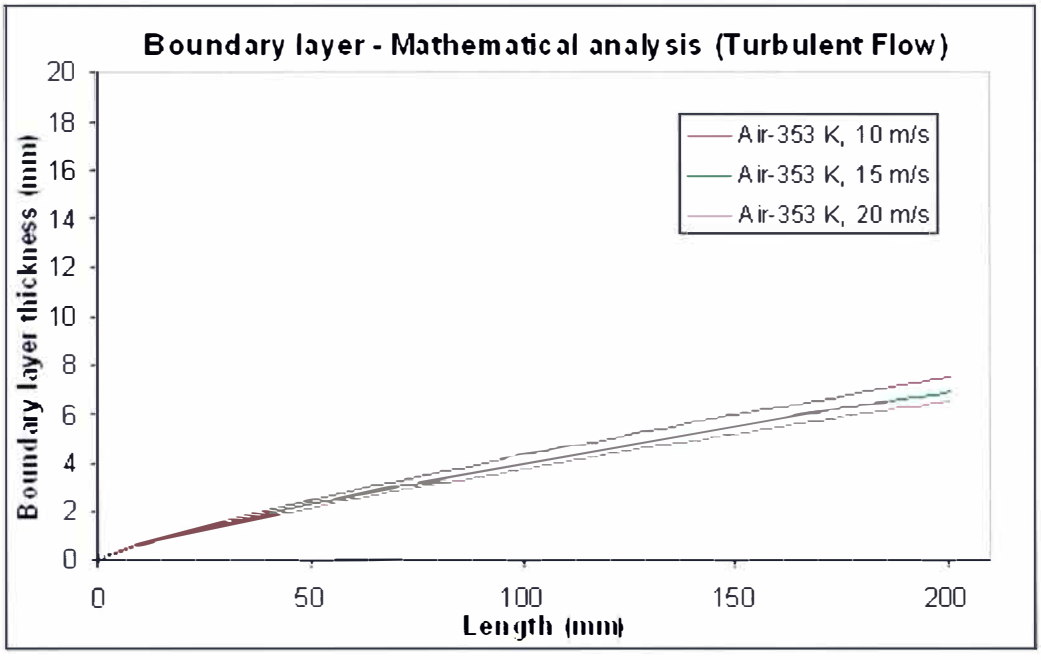

Figure 4.10 Theoretical boundary layer development along the flow geometry given by Equation (4.7) – Air, 353 K at 10 m/s, 15 m/s and 20 m/s

2-D Mathematical Analysis – Laminar Forced Convection

The Nusselt number for laminar forced convection flow on a flat plate with unheated starting length (x0) is given by Equation (4.9) [31].

$$Nu_x = \frac{0.453 \cdot \mathrm{Re}_x^{1/2} \cdot \mathrm{Pr}^{1/3}}{[1-(x_0/x)^{3/4}]^{1/3}} \qquad (4.9)$$

CFD analysis for laminar forced convection through the 2-D rectangular duct geometry (Refer Figure 4.4) was conducted for air at 353 K and for a heat flux of 400 W/m^2. A low inlet velocity of 0.5 m/s was used in order to achieve laminar flow conditions. The local Nusselt number comparison between CFD and analytical solutions (Equation (4.9)) is shown in Figure 4.11.

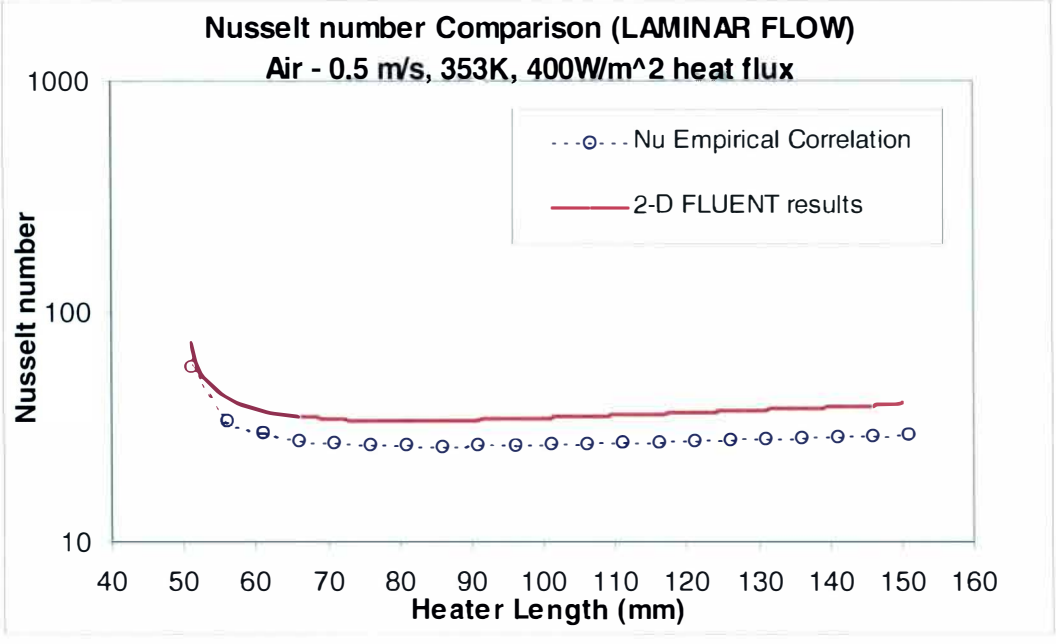

Figure 4.11 Nusselt number Comparison – CFD vs Eqn (4.9) results, Air 0.5 m/s, 353K, 400 W/m^2 heat flux (log scale) – Laminar flow

The comparison study showed that the 2-D computational results were more than 20% away from that of the analytical solutions obtained using Equation (4.9) for laminar forced convection. In this laminar internal flow, the thermal boundary layer develops well at the low velocity (0.5 m/s) and is not independent of the top wall of the flow geometry as in the case of turbulent flow through the 2-D rectangular flow channel. Hence the assumption of external flow, forced convection on a flat plate does not hold good for laminar flows in the 2-D flow channel. This leads to the deviation of analytical Nusselt number values from that of the computational results as expected. Figure 4.12 shows the laminar forced convective flow in the 2-D rectangular duct at 400 W/m^2 heat flux for air entering at 353 K and 0.5 m/s velocity (Also, refer Figure 4.9).

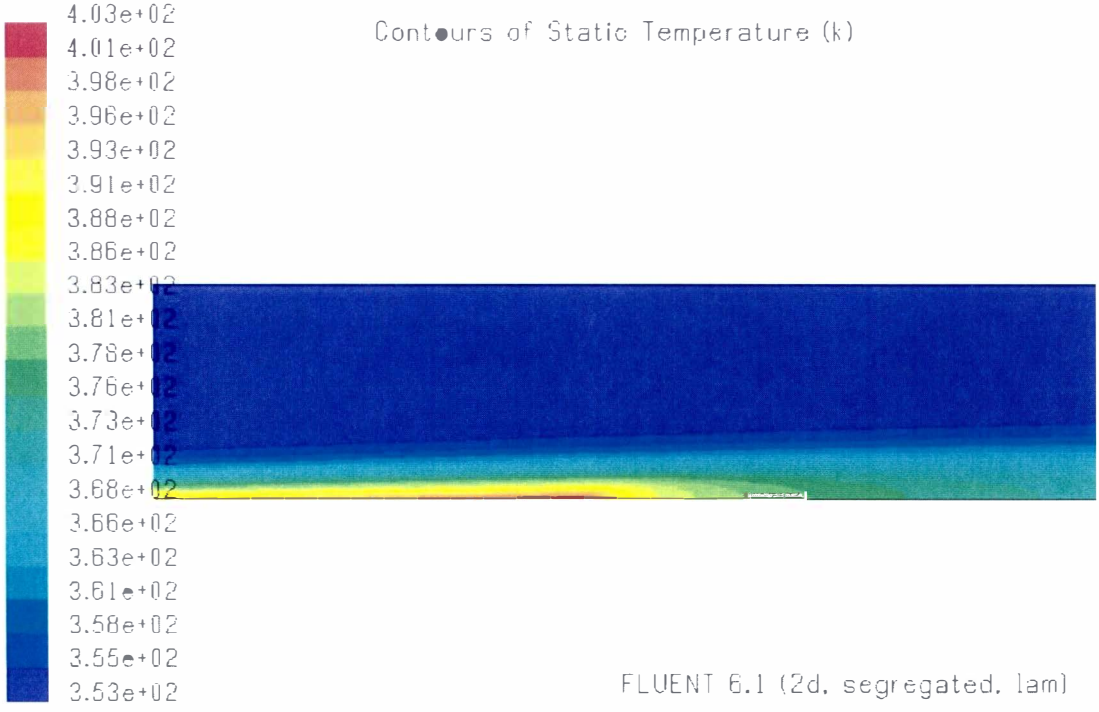

Figure 4.12 Laminar forced convection in the rectangular flow channel for air at 353 K, 0.5 m/s velocity, 400 W/m^2 heat flux

Hence, it was studied that forced convection on a flat plate with unheated starting length assumption can be applied only to turbulent flows in the flow loop rectangular test section and does not hold good for laminar flows marked by low velocities.

CHAPTER 5

RESULTS AND DISCUSSION

Temperature Distribution in the Flow Geometry

A three dimensional CFD analysis of the rectangular channel flow loop test section was carried out using FLUENT 6.1 software and the contours of static temperature for the half, symmetrically-cut flow geometry for 1 m/s velocity, 90°C inlet conditions of water is shown in Figure 5.1. A constant heat flux of 60650 W/m^2 was applied to the heater base.

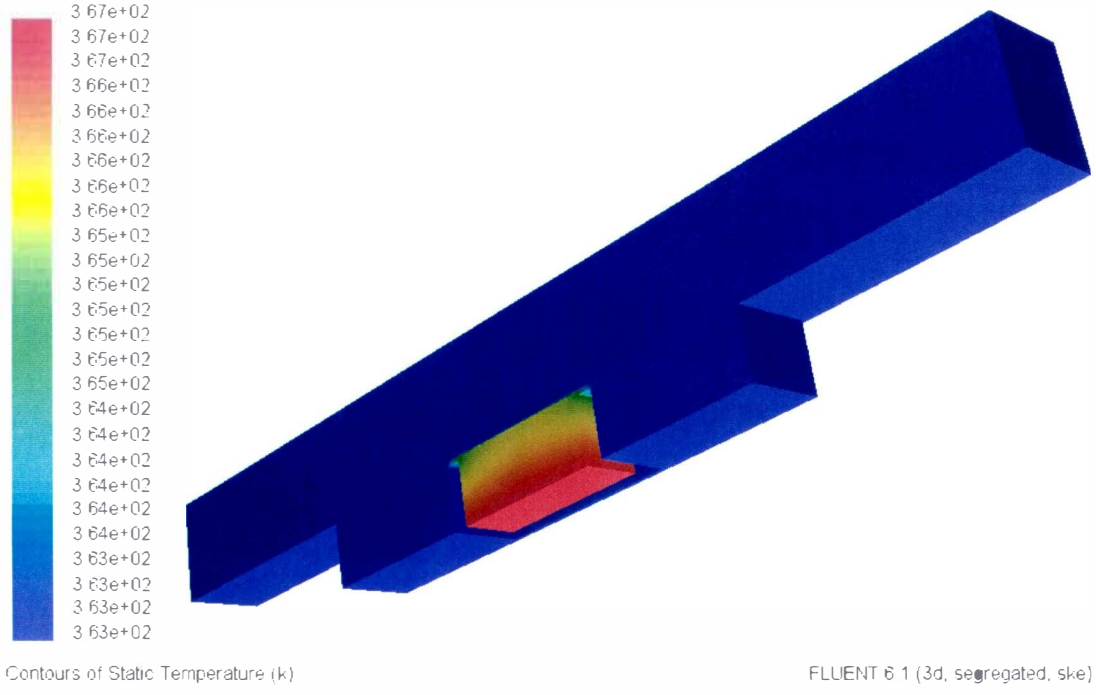

Figure 5.1 Temperature distribution in the flow assembly - 1 m/s, 90°C at 60650 W/m^2

There was not any significant change in the water temperature in the flow channel except near the heater surface. So, the inlet temperature (T_{in} = 90°C) was assumed to be the bulk temperature of the fluid (T_f). The constant heat flux applied to the base of the heater is conducted through its thickness and single phase forced convective heat transfer takes place at the heater surface. The temperature distribution on the surface of the heater in contact with the fluid is given in Figure 5.2.

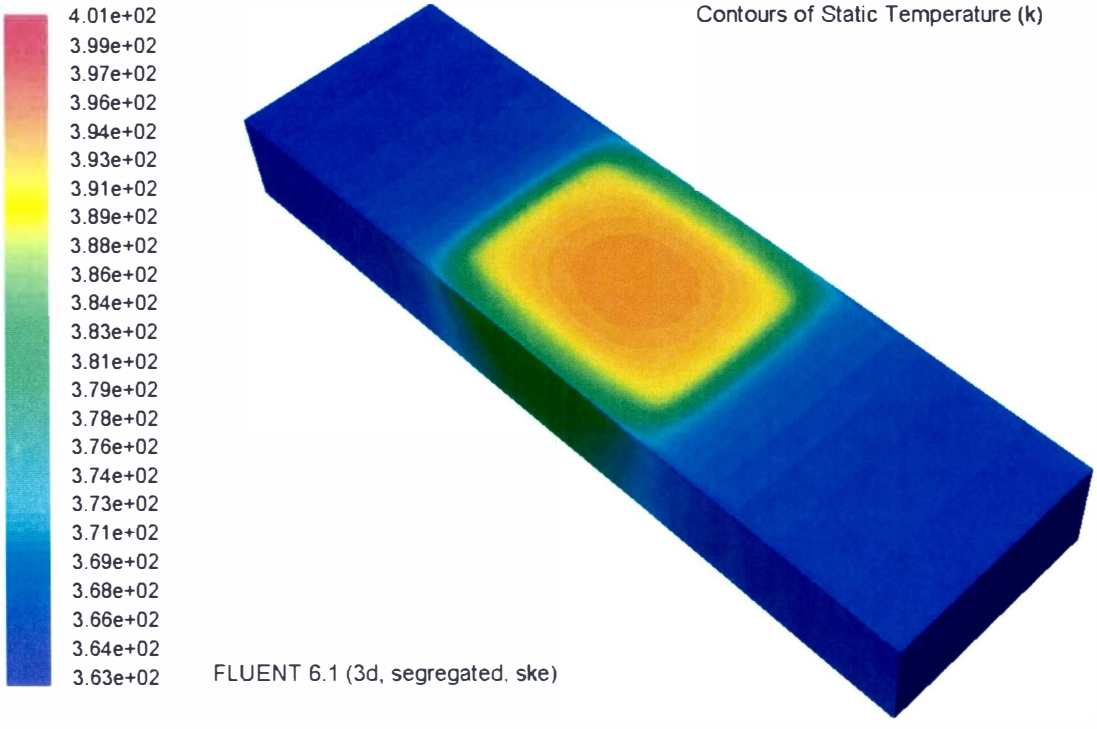

Figure 5.2 Temperature distribution on the heater surface- 0.5 m/s, 90°C at 293010 W/m^2

The FLUENT plot for temperature distribution on the surface of the heater indicated that there is heat leakage taking place through the four sides of the heater and the highest temperature point at the surface of the copper heater was at its center

(T_s or T_{wall}). The temperature gradient shown in Figure 5.2 is for water at 0.5 m/s velocity and at a heat flux of 293010 W/m^2. For lower heat fluxes and higher velocities, the temperature gradient at the heater surface would be lesser.

Heater Surface Temperature Study

The temperature distribution along the heater surface centerline for 1m/s velocity and 60650 W/m^2 heat flux is plotted in Figure 5.3.

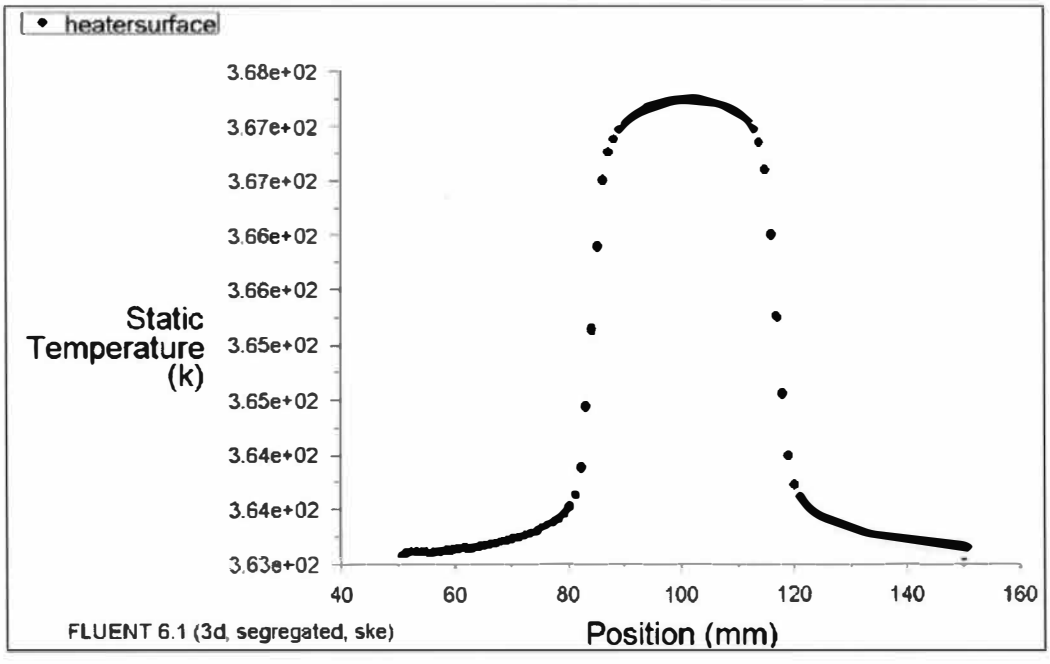

Figure 5.3 Temperature distribution along heater surface centerline
1 m/s, 90°C, 60650 W/m^2

The copper heater consists of 35 mm long unheated region followed by a 30 mm long heating section. Water entering at 363K (90°C) at the inlet is gradually heated along the length of the heater and reaches the highest temperature at the center point of the heater surface (at 100 mm). Then the temperature of water decreases

along downstream of the heater surface until it reaches the bulk fluid temperature (T_f = 363K). It should also be noted that the rise and fall in the heater surface temperature is not identical.

In Lee and O'Neill experimentation, based on the linear assumption between the thermocouple points T4 and T2, the surface temperature (T_s or T_{wall}) at the center point of the heater surface was calculated by extrapolation. In the 3-D computational analysis using FLUENT, temperatures at any location within the copper heater and the flow channel can be calculated using the Surface-Point command [22]. Heater surface temperature comparison graphs drawn with T_s in x-axis and the corresponding heat flux values in y-axis for 0.5 m/s, 1.0 m/s and 2.0 m/s velocities of water are shown in Figure 5.4, Figure 5.5 and Figure 5.6 respectively.

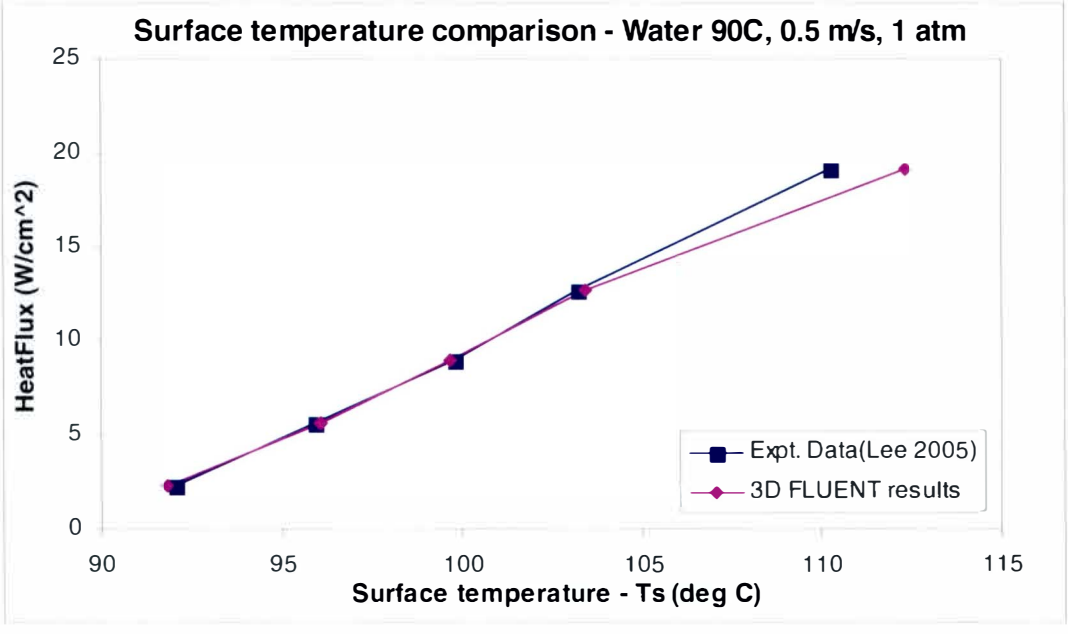

Figure 5.4 Surface temperature comparison – (CFD vs Experiment), water at 0.5 m/s

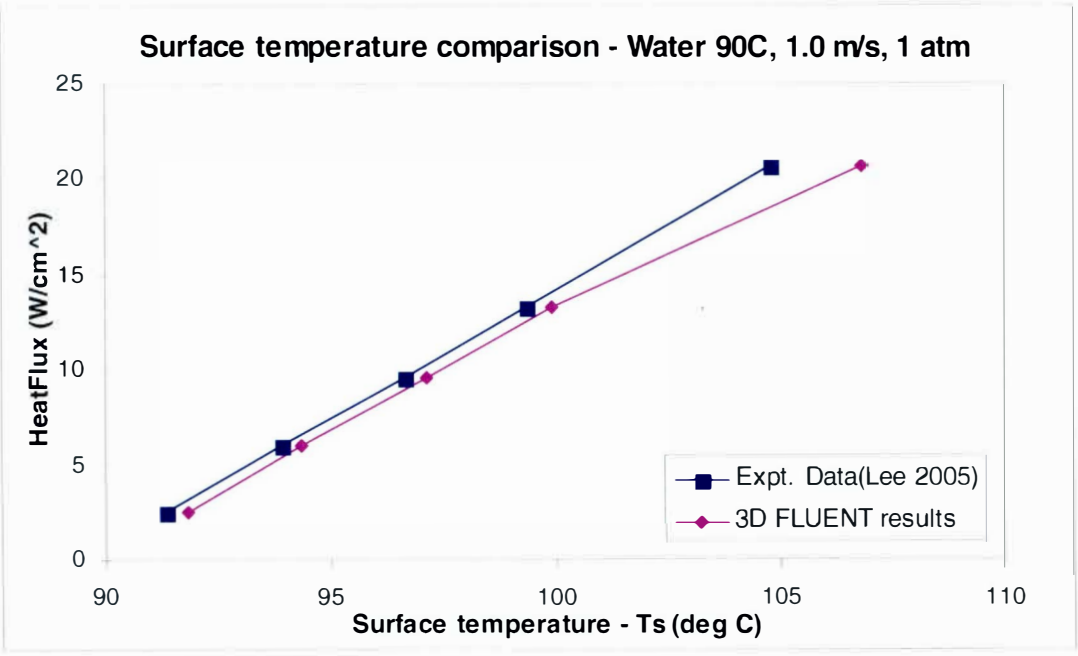

Figure 5.5 Surface temperature comparison – (CFD vs Experiment), water at 1.0 m/s

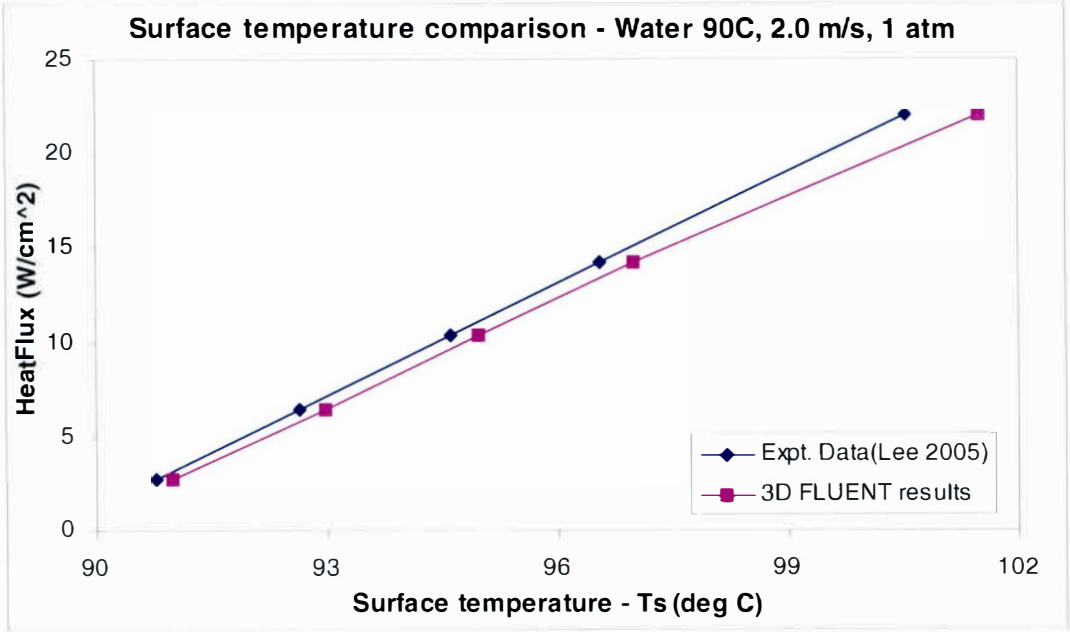

Figure 5.6 Surface temperature comparison – (CFD vs Experiment), water at 2.0 m/s

The wall temperatures at center of the heater surface obtained through computation and experimentation for different heat fluxes and velocities are listed in Table 5.1.

Table 5.1

Wall temperatures at center of heater surface– FLUENT vs Experiment

WATER 90°C, 1 atm Inlet velocity (m/s)	Heat flux (W/m^2)	Heater surface temperature T_{wall} (°C) **EXPERIMENT**	Heater surface temperature T_{wall} (°C) **FLUENT**
0.5	23280	92.0	91.8
	56150	95.8	96.0
	89830	99.7	99.6
	126170	103.1	103.4
	191400	110.1	112.2
1.0	25770	91.3	91.8
	60650	93.8	94.3
	133040	96.6	97.1
	284070	99.3	99.9
	375910	110.2	112.2
2.0	27720	90.8	91.0
	65060	92.6	92.9
	103470	94.6	95.0
	142450	96.5	97.0
	220860	100.5	101.4
	303030	104.4	106.4

In CFD analysis using FLUENT, adiabatic thermal condition was used for the heater sidewalls based on the assumption that the heat loss from the copper heater to the atmosphere is negligible. The 3-D computational heater surface temperature ($T_{s)}$ results showed reasonable agreement with the experimental data and it was noted that the CFD T_s values were slightly higher than that of the experimental results. This could be because of the adiabatic heater walls assumption used in FLUENT analysis. Since heat loss from copper heater to the surrounding air takes place in real experimentation by natural convection, the experimental surface temperatures (T_s) were slightly less compared to the computational 'T_s' values (Refer Figure 5.7). At higher heat fluxes (beyond 200000 W/m^2), boiling heat transfer takes place, which leads to further deviation of the single-phase CFD simulation results from the experimental data.

Heat Transfer Coefficient Comparison – CFD and Experimental Data

In 3-D computational analysis, based on the wall temperatures shown in Table 5.1, the heat transfer coefficient (h) was calculated using the general formula:

$$h = \frac{q''}{(T_w - T_f)} \tag{5.1}$$

where, T_w is the wall temperature at center of heater surface, T_f = 90ºC is the bulk fluid temperature and q'' is the heat flux applied to the base of the copper heater. To better understand the single-phase heat transfer characteristics on the heater surface, a graph between heat transfer coefficient (W/m^{2}K) and heat flux (W/cm^2) for different inlet velocities of water at 90ºC was plotted as shown in Figure 5.7.

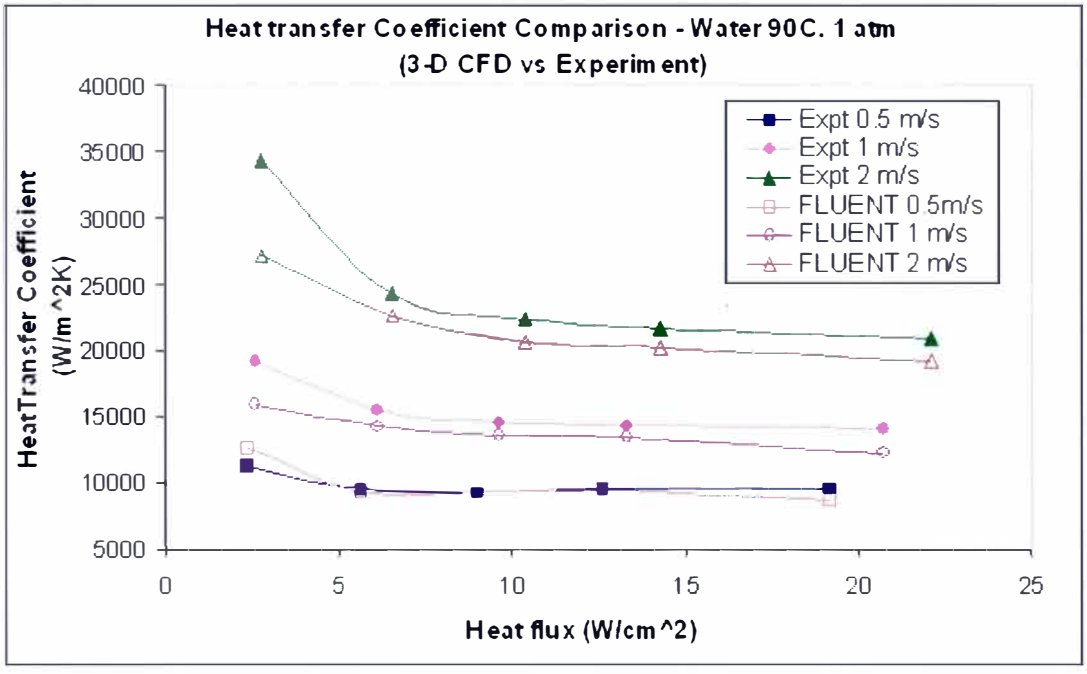

Figure 5.7 Heat transfer coefficient Comparison – CFD and experiment data
Water, 90°C at 0.5 m/s, 1.0 m/s and 2.0 m/s inlet velocities

It was seen that the heat transfer coefficient and hence the single-phase heat transfer is highly dependent on velocity and was increasing as the velocities were increased. Also, the heat transfer coefficient graph tends to become horizontal as the heat flux was increased. This showed that single-phase heat transfer is characterized by constant heat transfer coefficient values. During comparison between the numerical and experimentation heat transfer coefficients, high percentage error was noted for the lowest heat flux value at all inlet velocities of water. The error percentage was comparatively less and reasonably good at rest of the heat fluxes. In experimentation, based on the assumption of linearity between the thermocouples T_2 and T_4, the wall temperatures are obtained by extrapolation. In reality, the heat transfer from the heater base to its surface is not linear. This could be a reason for the error between wall temperatures and heat transfer coefficients of computational and

experimental analysis. For higher heat fluxes, the percentage error is high due to boiling heat transfer. The percentage error in comparison between CFD and experimental heat transfer coefficients for different velocities and heat flux values are given in Table 5.2.

Table 5.2

Percentage error in heat transfer coefficients – CFD vs Experimental results

Water 90C,1atm Inlet velocity (m/s)	Heatflux (W/m^2)	% error in heat transfer Coeff. comparison(h) (CFD vs Experiment)
0.5	23280	12
	56150	2
	89830	1
	128170	2
	191400	9
1.0	25770	17
	60650	8
	133040	7
	284070	6
	375910	12
2.0	27720	21
	65060	7
	103470	7
	142450	6
	220860	8

Heater Surface Temperature Profile for Different Heat Fluxes

Experimental analysis is restricted to study of temperatures at fixed points (T1, T2, T3 and T4). In CFD analysis using FLUENT, temperature profiles could be studied at any location in the flow domain. For water at 90°C and 0.5 m/s inlet velocity, the temperature profile along the center of the heater surface was obtained

from FLUENT for different heat fluxes and is shown in Figure 5.8. There is increase in the wall temperature with increase in heat fluxes applied to the heater base and it is also noted that the temperatures downstream of the heater surface was slightly higher than that of the upstream temperatures.

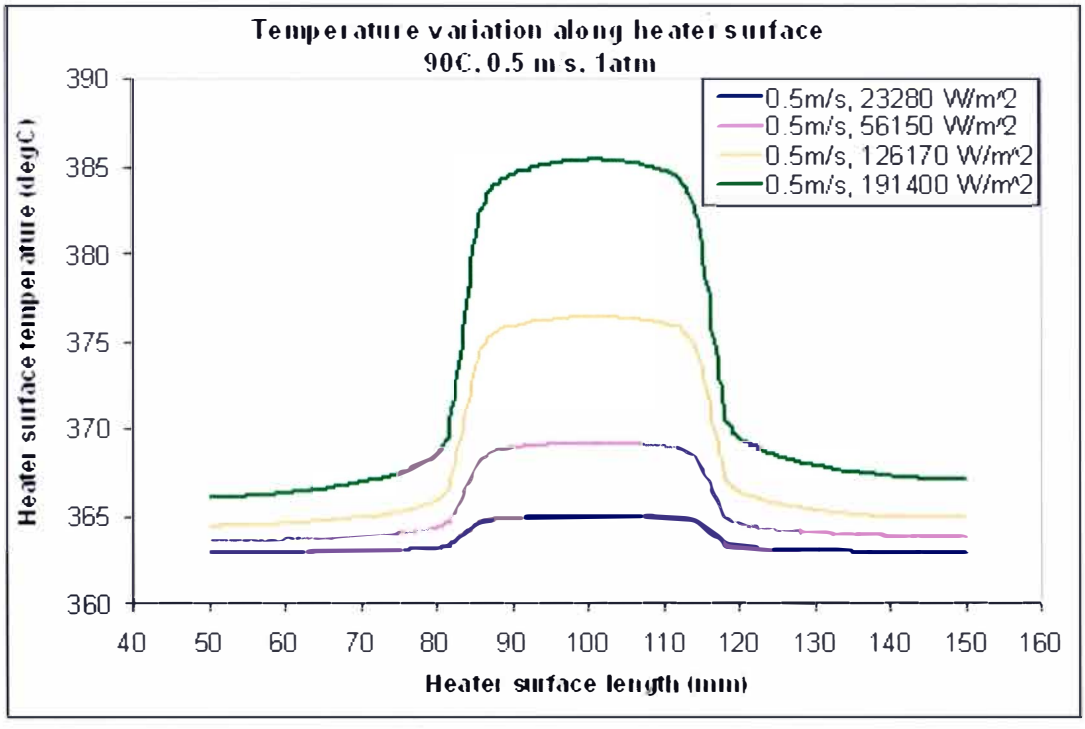

Figure 5.8 Temperature distribution along the heater surface center – water 90°C, 0.5 m/s

Nusselt Number Variation along the Heater Surface

Since the wall temperatures along the heater surface center are known from CFD simulations, the local heat transfer coefficients (h_x) along the heater surface are found using Equation (5.1). Once the heat transfer coefficients are known, the local Nusselt number distribution (Nu_x) along the heater surface can be calculated using

Equation (5.2).

$$Nu_x = \frac{h_x \cdot x}{k} \tag{5.2}$$

Here, x = 85mm to 115mm is the length of the heating region in the copper heater. Nusselt number variation along the heater surface for different heat flux values with water entering at 0.5 m/s velocity at 90°C is given in Figure 5.9.

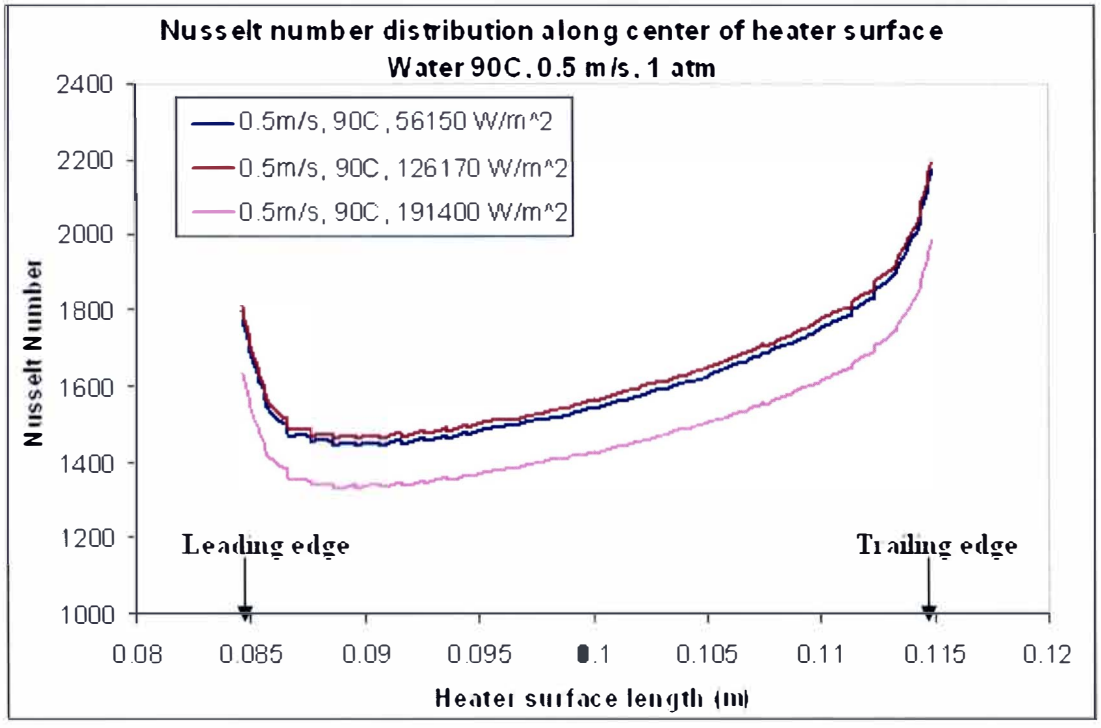

Figure 5.9 Nusselt number variation along center of heater surface- water 90°C, 0.5 m/s

It was noted that the local Nusselt number variation along the heater surface was very similar for both the heat fluxes, 56150 W/m^2 and 126170 W/m^2. This clearly indicated that the Nusselt number profile does not change with increase in heat fluxes

but remain constant for single-phase heat transfer conditions. When a higher heat flux (191400 W/m^2) was used, boiling starts to occur which changes the local Nusselt number profile as shown in Figure 5.9.

Thermal Boundary Layer – CFD Analysis

Heat transfer taking place along the center of the copper heater from heater base to its surface was studied using FLUENT and the temperature distribution along the heater's center is given in Figure 5.10.

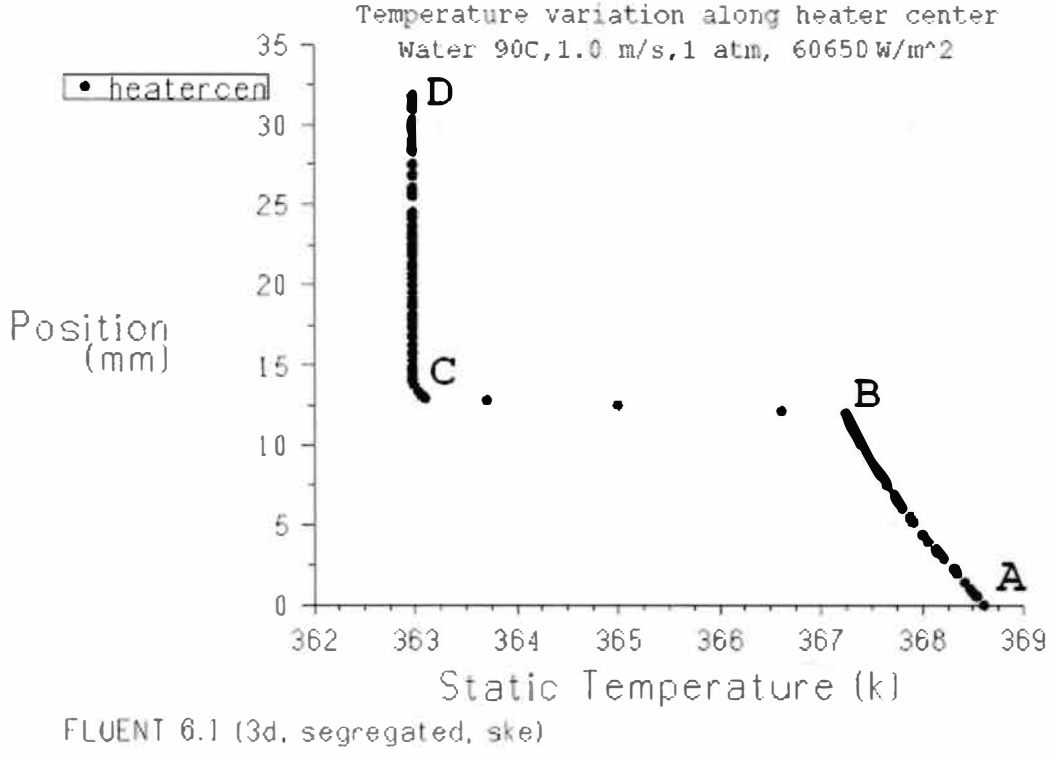

Figure 5.10 Temperature variation along copper heater center - 1m/s, 90C, 60650W/m^2

The temperature variation graph along the heater center can be divided in to three regions namely, AB, BC and CD. Along the 12mm thick heater, conduction heat transfer takes place (region AB) followed by thermal boundary layer development (region BC) because of forced convection between the heater surface and the fluid. Region CD in Figure 5.10 indicates that there is no change in the bulk temperature of the fluid (T_f) beyond the boundary layer and remains the same as that of the inlet fluid temperature ($T_f = T_{inlet} = 90°C$).

The thermal boundary layer on the heater surface (Refer Figure 5.10, region BC) for different inlet velocities and heat fluxes was obtained from FLUENT and plotted in Figure 5.11. It is an expanded view of region BC in Figure 5.10.

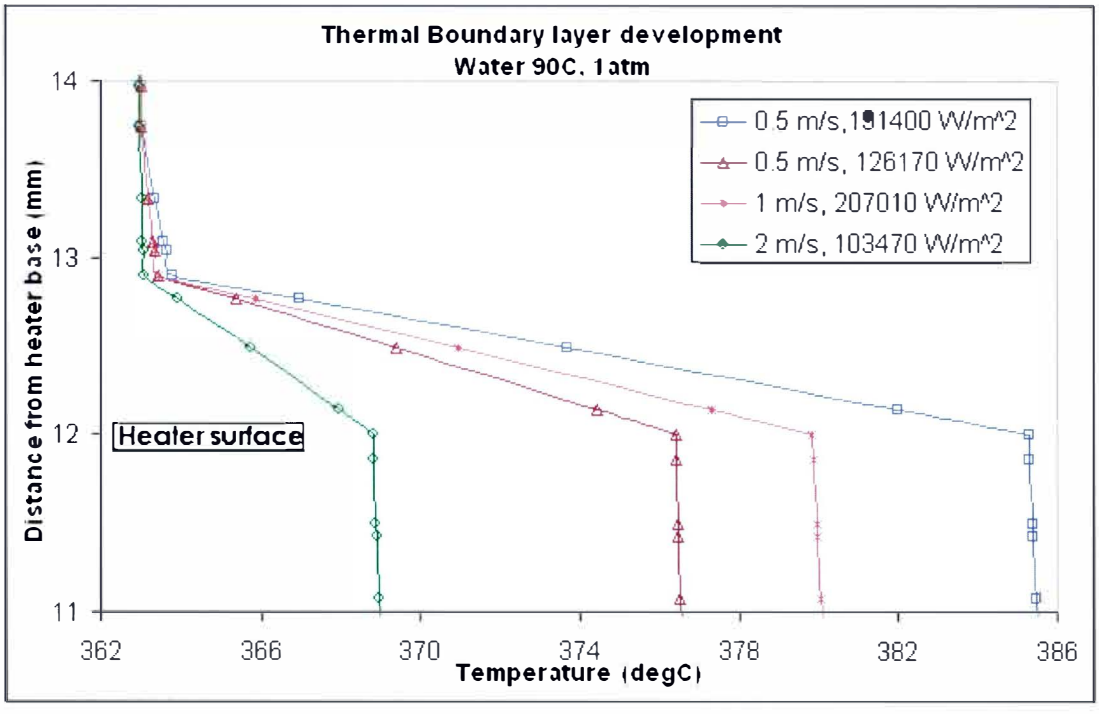

Figure 5.11 CFD Thermal boundary layer results- Water at 90°C - 0.5, 1, 2 m/s velocities

It was noted that the thermal boundary layer thickness (δ_T) was very thin (less

than 1 mm) for water even at a low velocity of 0.5 m/s and at high heat flux of 191,400 W/m^2. For higher velocities, the thermal boundary layer thickness would decrease further. The variation in the fluid temperature was seen only inside the thermal boundary layer and the fluid temperature was constant elsewhere ($T_f = 363K$).

CHAPTER 6

CONCLUSION

The single-phase, turbulent forced convection in the entry region of a rectangular duct was investigated computationally using FLUENT k- ε turbulence model. In the three-dimensional CFD analysis, the operating fluid is water at 90°C inlet temperature, 1 atm pressure and the inlet velocities are varied from 0.5 m/s to 2.0 m/s. The heat flux ranged from 0 W/m^2 to 200,000 W/m^2. The 3-D CFD results showed that the wall temperatures obtained on the surface of the heater increased with increase in the heat flux applied to the heater base. For the given heat flux, the highest temperature point at the surface of the heater was at its center. For different velocities of water, the wall temperature decreased with increase in inlet velocity. This indicates that the forced convection heat transfer on the heater surface increases with increase in velocity. It was clearly observed that the heat transfer coefficient was highly dependent on velocity, increasing as the velocity was increased. Also in single-phase forced convection, the heat transfer coefficients tend to become constant as the heat flux values were increased.

The 3-D numerical results showed good agreement with the experimental results of Lee and O'Neill (2005). Overall, the error percentage between the FLUENT and experimentation data for wall temperatures and heat transfer coefficient values was within 8%. It can be concluded that the FLUENT model developed in this study using the Standard k- ε turbulence model simulates the single-phase heat transfer mechanism in the flow loop test section of Lee and O'Neill [17, 18] with reasonable accuracy. A visual study of temperature distribution in the flow geometry obtained

from numerical simulation for different velocities and heat fluxes indicated that there is drastic change in the fluid temperature only at the vicinity of the heater surface and the fluid temperature does not change elsewhere. In the 3-D CFD study, the thermal boundary layer developed on the heater surface was very thin (less than 1 mm) for different heat fluxes and velocities of water. For a given velocity and heat flux, the temperature profile along the heater surface obtained from FLUENT showed that the wall temperature is increasing along the leading edge of the heater, reaches the highest temperature at the center and starts dropping along the trailing edge of the heater. Because of the direction of the fluid (from left to right), the wall temperatures along the trailing edge were slightly higher than that of the leading edge wall temperatures. For a given velocity, the local Nusselt number distribution along the heater surface was independent of heat flux and did not change with increasing heat fluxes.

A two-dimensional CFD analysis of turbulent forced convection in the rectangular flow channel was performed which showed that the 2-D flow loop test section could be mathematically modeled using the analytical solutions for turbulent forced convection on a flat plate with unheated starting length. For turbulent flows with high velocities in the rectangular duct, the thermal boundary layer developed is very thin and is independent of the top wall of the duct. In the 2D numerical simulation, the operating fluid is air at 80°C and the inlet velocities ranged from 10 m/s to 15 m/s. At 400 W/m^2 heat flux, the local Nusselt number variation along the heater length obtained from 2-D CFD analysis and the Nusselt number empirical correlation for turbulent forced convection on a flat plate [31] were compared. The CFD results showed good agreement with the empirical correlation and hence, it can be concluded that the turbulent forced convection in the 2-D flow loop test section is

analogous to turbulent flow over a flat plate with unheated starting length. This assumption did not hold good for laminar flows through the rectangular flow channel because at low velocities, the thermal boundary layer develops well and is not independent of the top duct wall. When a comparison of Nusselt number values between CFD data and empirical correlation for laminar forced convection was performed, the numerical simulation results showed more than 20% error.

By using the 3-D FLUENT model developed in this research, the effect of various parameters like velocity, pressure, inlet fluid temperature and heat flux on turbulent forced convection in the entry region of rectangular ducts could be studied. In this research, standard fluids like water and air were used for the turbulent forced convection study. Other pure fluids can also be analyzed using the existing FLUENT model. This model simulates only single-phase forced convection and does not include the effect of boiling. However, boiling heat transfer could be studied by incorporating User-Defined Functions (UDFs) [22] into the existing single-phase FLUENT model.

Appendix A

FLUENT - Velocity inlet boundary definition panel

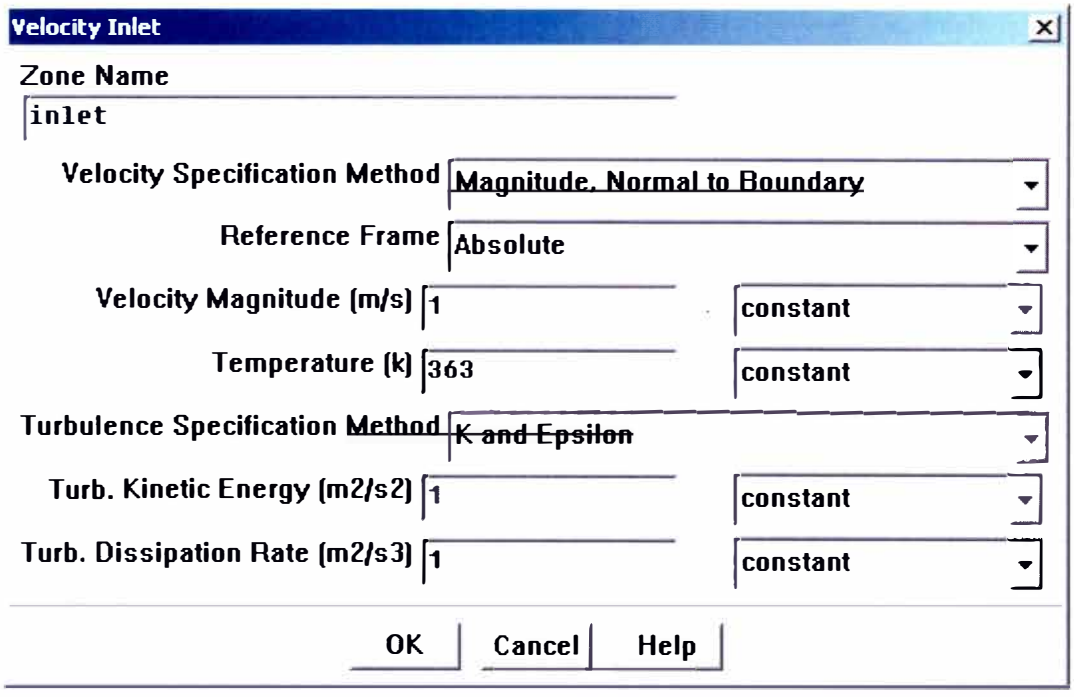

Figure A.1 Velocity inlet boundary definition in FLUENT

Appendix B

FLUENT – Turbulence model definition

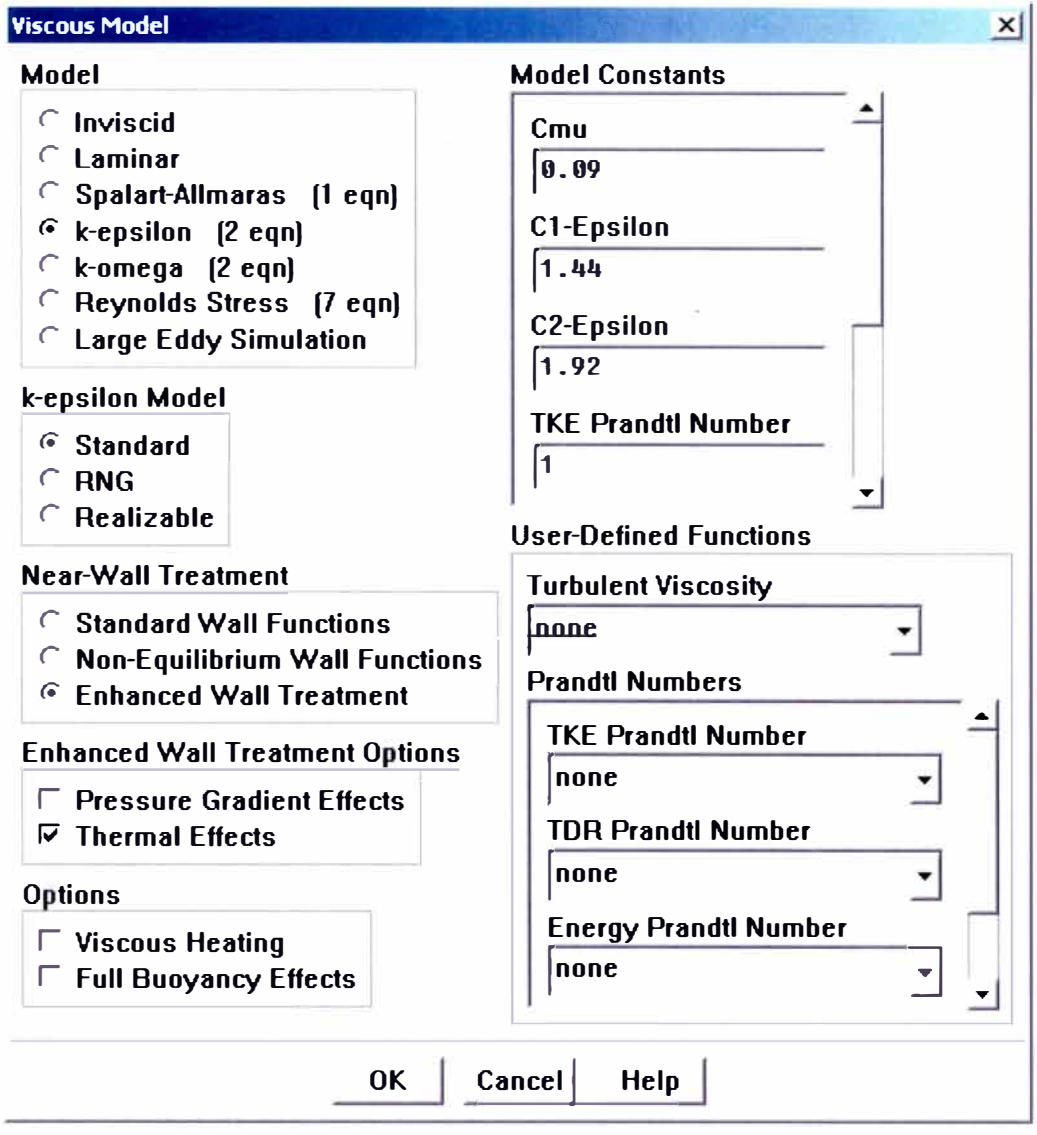

Figure B.1 k-epsilon turbulence model selection

BIBLIOGRAPHY

1. Fraas, Arthur P., "Heat Exchanger Design" (2nd Edition), Wiley-Interscience, New York, (1989), ISBN 0-471-62868-9

2. R.K Shah and A.L London, "Laminar flow forced convection in ducts", Adv. Heat Transfer Suppl. 1, Academic Press, New York (1978)

3. J.B. Aparecido and R.M. Cotta, "Thermally developing laminar flow inside rectangular ducts", Int. J. of heat & mass Transfer, vol. 33, No. 2, pp = 341 – 347 (1990)

4. Raja, A.V. et. al., "Heat transfer and fluid flow in a constructional heat exchanger", Proceedings of the 5nd International Conference on Enhanced, compact and ultra-compact heat exchangers, NJ, USA (Sep 2005)

5. Fakheri, A. Zhu, J., and Azeem, M., "Laminar developing flow inside heat conducting rectangular ducts", ASME Int. Mech. Engg. Congress & exhibition, Chicago-Illinois, USA (Nov 1994)

6. Chandrupatla, A.R., and Sastri V.M.K., "Laminar forced convection heat transfer of a non-Newtonian fluid in a square duct", Int. j. Heat & Mass transfer, vol. 20, page = 1313-1324 (1977)

7. Muzychka, Y.S., and Yovanovich, M.M., "Laminar forced convection heat transfer in the combined entry region of non-circular ducts", Journal of heat transfer, vol. 126, page = 54 – 61 (Feb 2004)

8. Bejan, A. and Kraus, A.D., "Heat Transfer handbook", John Wiley & Sons, Inc., New Jersey, (2003), ISBN 0-471-39015-1

9. Davis, S.J., and White, C.M., "An experimental study of the flow of water in pipes of rectangular section", Proc. Roy Soc., (A119): 92 – 107 (1928)

10. Allen, J. and Grunberg, N.D., "The resistance to the flow of water along smooth rectangular passages and the effect of a slight convergence and divergence of the boundaries", Philos. Mag., Ser.(7): 490 – 502 (1937)

11. Cornish, R.J., "Flow in a pipe of rectangular cross section", Proc. Roy. Soc. London, (A120): 691 – 700 (1928)

12. Harnett, J.P. and Koh, C.Y. and McComas, S.T., "A comparison of predicted and measured friction factors for turbulent flow through rectangular ducts", J. Heat Transfer, (84): 82 – 88 (1962)

13. Rao, "Friction factor and heat transfer coefficients for fully developed turbulent flow through axi-symmetrically heated rectangular ducts", USA.

14. Rokini, M., et all, "Numerical and experimental investigation of turbulent flow in a rectangular duct", Int. J. of Numerical Methods in fluids, vol. 28, page = 225 – 242 (1998)

15. Piller, M. and Nobile, E., "Direct Numerical Simulation Of Turbulent Flow And Heat Transfer In A Square Duct At Low Reynolds Number", 3rd Afosr International Conference On Dircet Numerical Simulation And Large Eddy Simulation (Taicdl), Texas, USA (2001)

16. Lee, H.S, and O'Neill, A., "Boiling curves and visual observations of subcooled flow boiling of water over a horizontal plate heater in a rectangular channel", Proceedings of the IMECE 2005, ASME Int. Mech. Engg. Congress and Exposition, Florida, USA (Nov 2005)

17. O'Neill, A., "Experimental determination of convective boiling curves for water and ethylene glycol in a rectangular channel with localized heating", Masters Thesis, Department of Mechanical Engineering, Western Michigan University (2005)

18. H. S. Lee and L. W. Cholewczynski, "A study on convection and boiling heat-transfer modes in a standard engine cooling system", IMechE report no. C599/050/2003, (2003)

19. Lee, H.S, and O'Neill, A., "Comparison of boiling curves between a standard S.I engine and a flow loop for a mixture of ethylene glycol and water", SAE 2006-0101231, SAE International, USA (2006)

20. F. P. Incorpera and D. P. Dewitt, "Fundamentals of Heat and Mass Transfer" (4^{th} Edition), John Wiley & Sons, Inc., New York, (1996), ISBN 0-471-30460-3

21. Solidworks User Guide 2005

22. FLUENT User guide 5.1

23. B. E. Launder and D. B. Spalding, "Lectures in Mathematical Models of Turbulence", Academic Press, London, England (1972)

24. GAMBIT 2.2 Documentation – Modeling Guide

25. Schlichting. H., "Boundary layer theory", 6^{th} ed., Mc-Graw Hill, New York, USA (1968)

26. Colburn, A.P., Trans. Am. Inst. Chemical Engineering, vol. 29, page = 174 (1933)

27. Cxhilton, T.H., and A.P. Colburn, Ind. Eng. Chem., vol. 26, page = 1183 (1934)

28. Kakac, S., Yener, Y., "Convective Heat Transfer" (2nd Edition), CRC Press Inc., Florida, (1994), ISBN 0-8493-9939-4

29. Subramanian, S., "CFD modeling of compact offset strip-fin high temperature heat exchanger", Masters Thesis, Department of Mechanical Engineering, University of Nevada (2005)